Nano-Micro Letters
e-ISSN 2150-5551
CN 31-2103/TB
REVIEW
https://doi.org/10.1007/s40820-025-02053-z

Cite as
Nano-Micro Lett.
(2026) 18:229
Received: 24 September 2025
Accepted: 13 December 2025
© The Author(s) 2026

Inorganic High-Performance Fiber-Based Materials for Electromagnetic Interference Shielding: Fundamentals, Fabrications, and Emerging Applications

Sijie Qiao[1], Zhicheng Shi[1], Aixin Tong[1], Zhiyu Huang[1], Annan He[1], Binhao Wang[1], Jun He[1], Jiaxin Wang[1], Ming Chen[1], Zixi Huang[1], Linhui Hao[1], Bing Wu[2], Yan Jun[1] ✉, Ya-Lan Tan[1] ✉, Pibo Ma[3] ✉, Weilin Xu[1], Fengxiang Chen[1] ✉

HIGHLIGHTS

- Inorganic high-performance fibers (IHPFs)-based composites development and electromagnetic interference (EMI) shielding mechanisms are reviewed.
- Surface modification strategies for IHPF's surface inertness challenge and EMI shielding layer construction are summarized.
- Future directions and current challenges for achieving large-scale, durable, and environmentally stable IHPF-based EMI shielding materials are outlined.

ABSTRACT Confronted with increasingly severe challenges of electromagnetic interference (EMI) and electromagnetic radiation pollution in industrial, military, and aerospace applications, the development of novel materials that combine high shielding efficiency with excellent comprehensive performance has become a research hotspot. Inorganic high-performance fibers (IHPFs), recognized for their lightweight nature, outstanding mechanical properties, and chemical stability, are regarded as ideal candidate materials for designing lightweight, durable, and structurally functional integrated EM shielding systems. However, besides metal fibers, most IHPFs exhibit intrinsic surface chemical inertness and physical smoothness, resulting in poor interfacial compatibility and weak adhesion with functional coatings or resin matrices, which significantly undermine the long-term service reliability of composites under extreme conditions. This paper introduces the EM shielding mechanism, highlights common issues of surface inertness in IHPFs, and elaborates on both "dry" and "wet" surface modification strategies. These strategies enable the formation of robust functional layers, facilitating the integration of high strength, high modulus, and multifunctionality, while ensuring interfacial reliability in composites. Furthermore, the principles and processing techniques of various strategies for fabricating EMI shielding functional layers on IHPFs surfaces are reviewed, and recent advances in the application of functionalized IHPFs, as well as service reliability and environmental stability, are summarized, including EMI shielding protection and radar-absorbing stealth. Finally, the challenges and future research directions for the large-scale and long-term stable application of IHPF-based EMI shielding

✉ Yan Jun, yanjun98@wtu.edu.cn; Ya-Lan Tan, yltan@wtu.edu.cn; Pibo Ma, mapibo@jiangnan.edu.cn; Fengxiang Chen, fxchen_czx@wtu.edu.cn
[1] State Key Laboratory of New Textile Materials and Advanced Processing, Wuhan Textile University, Wuhan 430200, People's Republic of China
[2] China Coal Technology & Engineering Group (CCTEG), Chinese Institute of Coal Science (CICS), Beijing 100013, People's Republic of China
[3] Engineering Research Center of Knitting Technology, Ministry of Education, College of Textile Science and Engineering, Jiangnan University, Wuxi 214122, People's Republic of China

Published online: 30 January 2026

functionalization in high-end fields are discussed, offering insights that may accelerate the development of next-generation lightweight, sustainable, and multifunctional EMI shielding materials.

KEYWORDS Inorganic high-performance fibers/fabrics; Electromagnetic shielding; Mechanism; Atomic layer deposition; Electromagnetic protection; Future challenges

Abbreviations

EM	Electromagnetic
EMI	Electromagnetic interference
EMR	Electromagnetic radiation
IHPF	Inorganic high-performance fiber
ALD	Atomic layer deposition
CVD	Chemical vapor deposition
SE_R	Reflection loss
SE_M	Multiple reflection loss
SE_A	Absorption loss
SE_T	Total EM shielding effectiveness
VNA	Vector network analyzer
SSE	Specific shielding effectiveness
LIG	Laser-induced graphene
GF	Glass fiber
CF	Carbon fiber
BF	Basalt fiber
QF	Quartz fiber
SiC	Silicon carbide
Al_2O_3	Aluminum oxide
PECVD	Plasma-enhanced chemical vapor deposition
VG	Vertical graphene
CNTs	Carbon nanotubes
MWCNTs	Multiwalled carbon nanotubes
AZO	Aluminum-doped zinc oxide
TMA	Trimethylaluminum
AgNWs	Silver nanowires
ScPEG	Solid–solid phase change polyethylene glycol
IFSS	Interfacial shear strength
ILSS	Interlaminar shear strength
HMCF	High-modulus carbon fiber
LMs	Liquid metals
ANF	Aramid nanofiber
Co–Ni	Cobalt–nickel
ACBF	Aramid-carbon blended fabric
xGnPs	Exfoliated graphene nanoparticles
PPy	Polypyrrole
PANI	Polyaniline
PTh	Polythiophene
PDA	Polydopamine
RL_{min}	Minimum reflection loss
VARI	Vacuum-assisted resin infusion
MOFs	Metal–organic frameworks
MXenes	Two-dimensional transition metal carbides and nitrides
VSS	Vapor-surface–solid
VS	Vapor–solid
GO	Graphene oxide
AF	Alumina fiber
g_s	Green shielding index
RCS	Radar cross-section
PAN	Polyacrylonitrile
EAB	Effective absorption bandwidth
DEZ	Diethylzinc
CTE	Coefficient of thermal expansion

1 Introduction

With the rapid development of wireless communication, radar technology, and the widespread use of gigahertz power devices, the space we live in has become saturated with dense EM waves. The resulting electromagnetic interference (EMI) and electromagnetic radiation (EMR) pollution have emerged as significant issues that cannot be ignored. They not only lead to malfunctions of precision electronic devices and jeopardize information security, but also pose potential threats to human health [1–3]. In extreme environments such as aerospace, additional natural factors including strong ultraviolet radiation and cosmic rays further affect the orderly operation of space stations and the health of astronauts. Traditional metallic shielding materials (e.g., copper and aluminum foils), though exhibiting excellent electrical conductivity and shielding performance, suffer from inherent drawbacks such as high density, susceptibility to corrosion, rigidity, and poor processability. These limitations severely restrict their application in modern electronic devices that demand lightweight, flexible, and highly integrated materials [4, 5]. Consequently, it is urgent to develop high-efficiency, lightweight, and durable EMI shielding materials suitable for aerospace, military, and other extreme conditions.

Among the candidate materials, inorganic high-performance fibers (IHPFs) have attracted growing attention due to their unique structural and excellent comprehensive properties. Generally, IHPFs can be broadly classified into traditional IHPFs and emerging nanomaterial-based fibers. The traditional IHPFs include glass fibers (GFs), quartz fibers

© The authors https://doi.org/10.1007/s40820-025-02053-z

(QFs), basalt fibers (BFs), SiC fibers, and other ceramic fibers. Their high strength-to-weight ratios, excellent thermal stability, and remarkable chemical inertness make them ideal structural materials for aerospace and defense applications (Fig. 1 and Table 1) [6–8]. In contrast, the emerging nanomaterial-based fibers—such as carbon nanotube (CNT) fibers, graphene fibers, MXene fibers, and hybrid nanofibers—exhibit outstanding electrical conductivity, flexibility, and multifunctionality derived from their nanoscale building blocks [9–11]. However, except for metallic and carbon-based fibers [12, 13], most traditional IHPFs are insulating in nature, making it difficult to realize effective reflection and absorption of EM waves [14–16]. Moreover, these fibers share inherent challenges: their highly stable chemical structures and smooth surfaces result in low surface energy and a scarcity of reactive sites, which can easily lead to delamination of functional coatings under stress or thermal cycling, ultimately causing the loss of EMI shielding functionality. This has become a critical bottleneck affecting their functional modification and the overall performance of fiber-reinforced composites [17–19].

To overcome these intrinsic limitations of traditional IHPFs, surface activation and interfacial modification have become indispensable strategies. Addressing the surface inertness of IHPFs not only enables the construction of robust functional layers on their surfaces—integrating high strength, high modulus, and multifunctionality—but also promotes strong interfacial adhesion with various polymer matrices, ensuring excellent composite performance. Therefore, necessary surface activation pretreatments, aimed at increasing surface roughness and introducing reactive chemical groups, serve as the prerequisite and key initial step for building durable EMI shielding coatings. Considerable research has been devoted to improving fiber surface activity. Currently, the most widely explored approaches include liquid-phase oxidation [20, 21], electrochemical oxidation [22, 23], plasma treatment [24, 25], surface sizing [26, 27], coating [28, 29], and chemical grafting [30, 31]. Although electrochemical oxidation has been extensively applied in industry, harsh modification conditions may impair fiber mechanical properties. Plasma treatment offers high efficiency, but entails high costs and potential surface damage. Surface sizing and coating methods, which apply a compatible polymer layer onto fiber surfaces, can effectively protect the fibers and are relatively simple, though they may encounter interfacial bonding issues with polymer matrices. Surface grafting, on the other hand, has emerged as an important strategy for fiber functionalization, offering strong design flexibility, controllable and mild reaction conditions, and minimal damage to fiber mechanical properties. However, challenges remain regarding the control of grafting degree and uniformity. Each method presents distinct advantages and disadvantages, requiring careful selection based on practical application needs.

After successful surface activation, precise functionalization strategies become critical for imparting EMI shielding and absorption capabilities to the fibers. The central objective of these strategies lies in constructing continuous conductive networks and incorporating magnetic or dielectric loss components. Conventional physical deposition and chemical treatment methods, as well as emerging interfacial modification techniques, represent the primary pathways. Physical deposition techniques such as magnetron sputtering [32–34], vacuum-assisted filtration [35, 36], and spraying [37, 38] can rapidly form metallic or carbon-based thin films on fiber surfaces, thereby enhancing conductivity and shielding performance, though challenges of adhesion and durability remain. In contrast, electroless plating [39–41], electroplating [42, 43], and chemical vapor deposition (CVD) [44–46] can produce dense, continuous metallic or carbon-based coatings with superior electrical conductivity and wear resistance. By tailoring parameters such as coating thickness, grain size, and interfacial morphology, the shielding mechanism—including reflection, absorption, and multiple scattering—can be finely regulated. Additionally, in situ polymerization [47–49] and surface grafting [50, 51] can introduce conductive polymers (e.g., polyaniline, polypyrrole) onto fiber surfaces, yielding lightweight, flexible composites that balance mechanical integrity with EM loss performance. In recent years, with advances in nanotechnology, novel strategies such as atomic layer deposition (ALD) [52–54] and laser etching [55, 56] have been increasingly applied to the functional modification of IHPFs. ALD, with its atomic-level precision in layer-by-layer deposition, enables the formation of uniform, ultra-thin, and strongly adherent conformal coatings, providing new opportunities for interfacial engineering and multifunctional integration. Laser etching, by directly creating micro–nano-structures on fiber surfaces, enhances interfacial roughness and increases multiple scattering pathways of EM waves, thereby significantly improving absorption performance. Taken together, the continuous evolution of surface functionalization strategies is offering greater design flexibility and

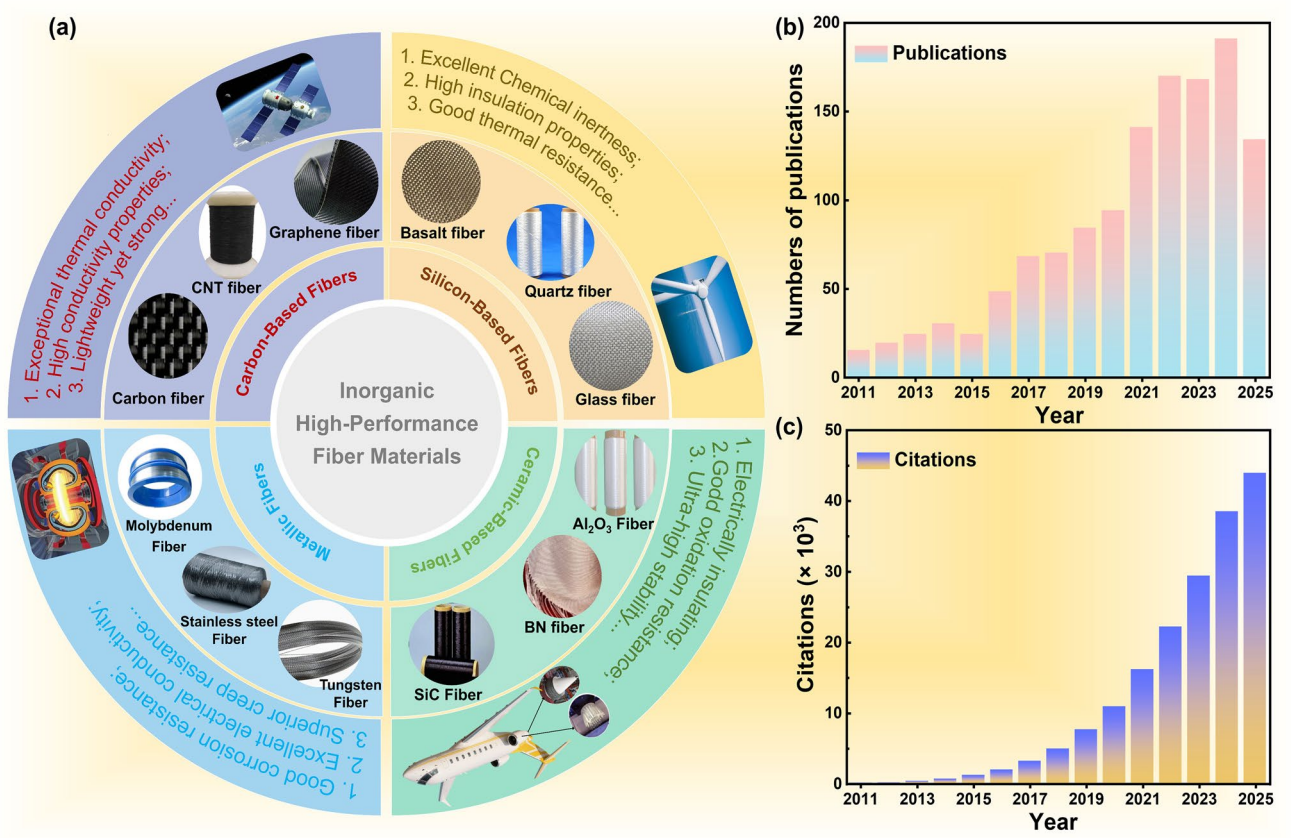

Fig. 1 **a** Inorganic high-performance fiber materials used in EMI shielding with their corresponding functional characteristics. **b, c** Numbers of publications and citations regarding IHPF materials with EMI shielding properties from 2011 to 2025. The data were collected on the Web of Science with the key words of "Carbon fiber", "Graphene fiber", "CNT fiber", "Basalt fiber", "Quartz fiber", "Glass fiber", "SiC fiber", "BN fiber", "Al_2O_3 fiber", "Molybdenum fiber", "Tungsten fiber", "Stainless steel fiber", and "EMI Shielding"

broader application prospects for IHPF-based EMI shielding materials.

Although significant progress has been achieved in the study of IHPFs for EMI shielding, there is still a lack of systematic reviews summarizing their preparation methods, application scenarios, and future challenges. This review aims to fill that gap by providing a comprehensive overview of this rapidly evolving field. First, the mechanisms of EMI shielding and corresponding evaluation criteria are discussed. Then, the inherent challenges of IHPFs are analyzed, along with current approaches to overcome them and their respective advantages and limitations. Subsequently, we focus on the functionalization strategies for imparting EMI shielding properties to IHPFs, covering both traditional physical and chemical methods as well as emerging interfacial modification techniques. Furthermore, their innovative applications in extreme environments such as aerospace, advanced electronics, and stealth defense are elaborated. Finally, the major challenges and future directions in this field are outlined, aiming to provide valuable insights and inspiration for the design of the next generation of structurally integrated, multifunctional EMI shielding materials.

2 Fundamental Principles for Electromagnetic Shielding

2.1 Electromagnetic Shielding Mechanisms

Shielding refers to the suppression of EMI by "cutting off" the coupling paths of EM fields, and it is one of the primaries means of achieving protection against EM radiation. EM shielding involves the use of conductive or magnetic materials to confine EMR within a specified spatial region. The purpose is either to enclose the interference source with a shielding body to suppress its disturbance to sensitive

© The authors https://doi.org/10.1007/s40820-025-02053-z

Table 1 Mechanical and physical properties and applications of IHPFs

Fiber category	Fiber types	Key characteristics	Main applications	References
Carbon-based fiber	CF	Ultra-high specific strength; Good fatigue resistance; Excellent electrical conductivity	Aircraft & spacecraft structures, sporting goods	[54]
	Graphene fiber	Lightweight yet strong; Superior flexibility; Outstanding EMI shielding ability	Wearable sensors, flexible supercapacitors, batteries	[100]
	CNT fiber	Outstanding specific strength; Low density; Ultra-high electrical conductivity	EMI shielding wires, flexible conductors	[99]
Silicon-based fiber	BF	Excellent thermal stability; Good flame retardancy; Environmentally friendly	Fireproof fabrics, sporting goods, wind blades	[95]
	GF	High tensile strength at low cost; Chemical inertness; Easy processability	Antenna covers, boat hulls, wind blades	[91]
	QF	Outstanding thermal shock resistance; Electrically insulating	High-frequency radomes, precision optical components	[92]
Ceramic-based fiber	SiC fiber	Outstanding oxidation resistance; corrosion-proof; Superior radiation resistance	Rocket nozzles, jet-engine hot-section parts (blades, vanes)	[105]
	Si_3N_4 fiber	Chemically inert; Outstanding neutron & radiation tolerance	Hypersonic vehicle radomes	[104]
	Al_2O_3 fiber	Ultra-high temperature stability; Low thermal conductivity; Chemical inertness	Furnace linings, metal-matrix brake pads, lightweight armor	[102]
	BN fiber	Low density & lightweight; Good flexibility & weaveability	Rocket combustion-chamber liners, antenna radomes	[103]
Metal fiber	Molybdenum fiber	Superior creep resistance; Good corrosion resistance Ideal for extreme-environment	High-temperature furnace elements, hypersonic thermal protection systems	[12]
	Tungsten fiber	Highest melting point; Low thermal expansion coefficient; Excellent electrical conductivity	Rocket nozzle reinforcements, radiation shields	[13]

equipment or to protect personnel in the surrounding space, or to enclose sensitive equipment to prevent interference from external sources. In general, EMI shielding refers to shielding against alternating EM fields above 10 kHz [57–60]. According to EM theory, in high-frequency EM waves characterized primarily by radiation, the electric and magnetic fields are interdependent. Therefore, in practice, shielding either the electric or the magnetic field is sufficient, since the other will be eliminated simultaneously.

The mechanisms of EMI shielding can be explained using various approaches, such as the eddy current effect method [61, 62], EM field theory, and transmission line theory. Among these, the transmission line theory has become widely adopted because of its computational simplicity, high accuracy, and intuitive understanding. As illustrated in Fig. 2a, transmission line theory treats the shielding body as a segment of a transmission line. When a radiation field encounters the shielding material, part of it is reflected at the outer surface, while the remainder penetrates into the shield and propagates forward [63–65]. During propagation, the EM waves undergo continuous attenuation within the shield, along with multiple reflections and transmissions at its interfaces. Therefore, the shielding mechanism comprises three components: reflection loss (SE_R) on the surface of the shield, absorption loss (SE_A) within the shielding material, and multiple reflection loss (SE_M) inside the shield.

Based on Schelkunoff's theory [66], the total EM shielding effectiveness (SE_T) can be expressed as the combined contribution of SE_R, SE_A, and SE_M for the EM waves transmitted through the shielding body, as shown in Eq. (1):

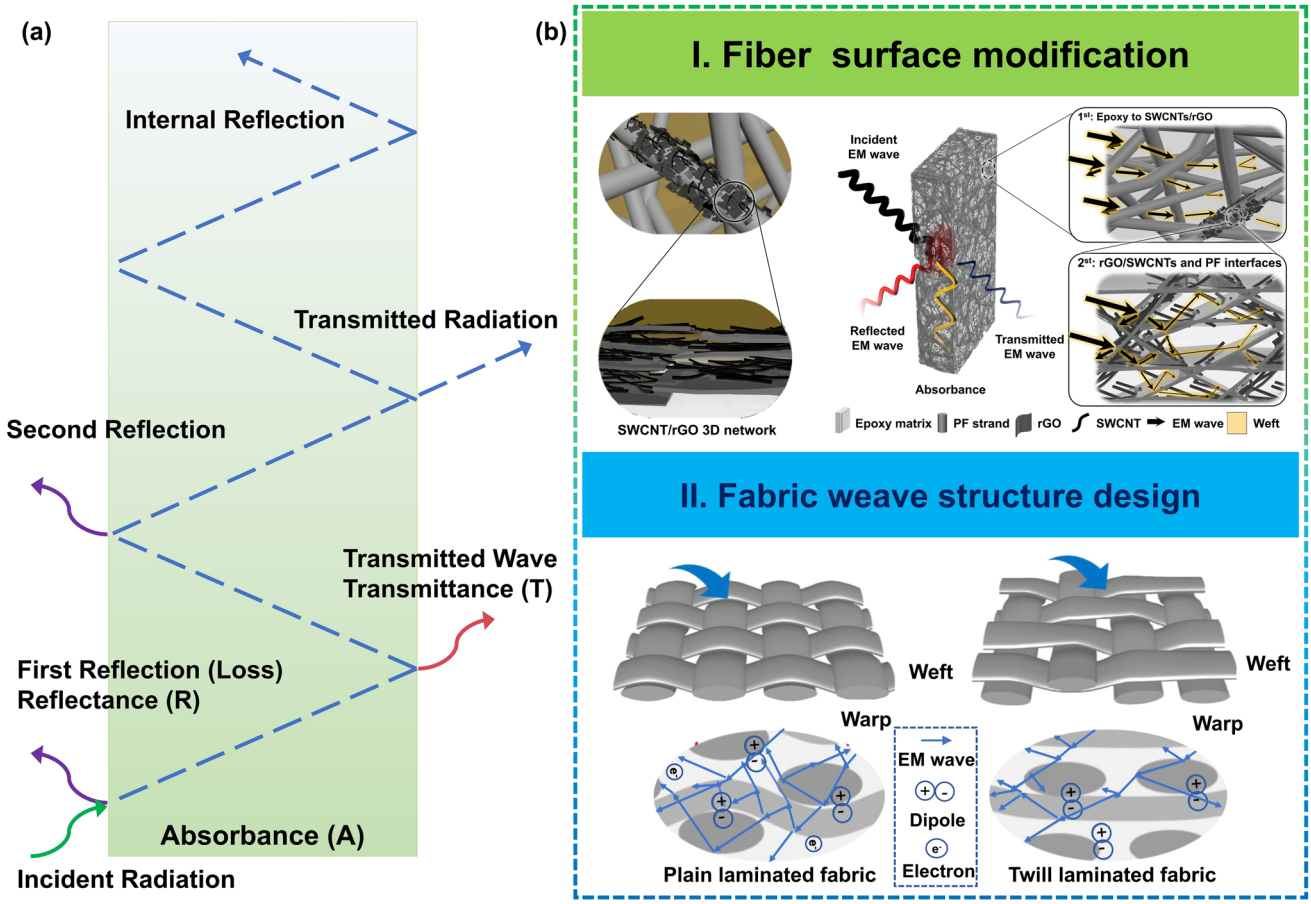

Fig. 2 Electromagnetic shielding mechanism. **a** Transmission line theory. **b** From fiber surface modification to fabric weave structure design. **I.** The EMI shielding mechanisms for the carbon ink-loaded PF/epoxy composites; **II.** Fabric weave structure design: EMI shielding mechanism of plain-weave structure and twill weave structure. Reproduced with permission from [85]. Copyright 2021, Elsevier B.V

$$SE_T = SE_R + SE_A + SE_M \quad (1)$$

The intensity of EM waves penetrating into a conductor decreases progressively with increasing depth. The skin depth (δ) is defined as the distance at which the EM waves intensity decreases to $1/e$ (e is the Euler's number; $1/e = 0.37$) [67–69]. The expression for δ is given as:

$$\delta = \frac{1}{\alpha} = \left(\sqrt{\pi f \sigma \mu}\right)^{-1} \quad (2)$$

Here, σ denotes the electrical conductivity, f the radiation frequency, and μ the magnetic permeability. The parameter α is the attenuation constant of EM waves in the shielding material, expressed as $\alpha = \omega\sqrt{\frac{\mu\varepsilon}{2}\left[\sqrt{1+\left(\frac{\sigma}{\omega\varepsilon}\right)^2}-1\right]}$, where ω represents the angular frequency ($2\pi f$) and ε the dielectric constant. From Eq. (2), δ decreases with increasing f, σ, and μ.

2.1.1 SE_R

The shielding effectiveness due to reflection arises from the impedance mismatch between the propagation medium of the incident EM waves and the surface of the shielding material. When an incident EM wave encounters a conductive material with high carrier density, a portion of the wave is reflected due to the discontinuity in the intrinsic impedance. Therefore, SE_R is primarily determined by the electrical conductivity and carrier mobility of the shielding material. The SE_R value from the front to the back surface of the shielding layer can be expressed as Eq. (3):

$$SE_R = 20\log_{10}\left(\frac{Z+Z_0}{4ZZ_0}\right) = 39.5 + 10\log_{10}\frac{\sigma}{2f\pi\mu} \quad (3)$$

Here, Z and Z_0 represent the impedances of the shielding material and air, respectively. According to Eq. (3), SE_R is related to the material's σ and μ as well as the frequency f of the EM waves [70].

2.1.2 SE_A

SE_A represents the attenuation of the EM waves energy as it propagates through the material. The incident wave induces eddy currents and dipole polarization losses within the shielding layer, which convert EM energy into heat [71]. To significantly enhance absorption loss, the following conditions are required: (i) high electrical conductivity for Ohmic loss, which strengthens the interaction between electrons and incident EM waves; and (ii) high σ and μ, which increase eddy current loss and hysteresis loss. The absorbed EM energy is dissipated in the form of heat. The SE_A of the shielding material can be expressed as Eq. (4):

$$SE_A = 20\left(\frac{d}{\delta}\right)\log_{10} e = 8.68\frac{d}{\delta} = 8.68d\sqrt{f\mu\sigma} \quad (4)$$

where d denotes the thickness of the shielding layer. Thus, SE_A depends on controllable parameters such as thickness and conductivity, as well as the intrinsic EM properties of the material.

2.1.3 SE_M

SE_M accounts for the energy dissipation caused by multiple internal reflections at interfaces or within porous/multilayer structure This process can repeat until the EM energy is fully dissipated. The multiple reflection efficiency (SE_M) of a shielding material is calculated as Eq. (5):

$$SE_M = 20\log_{10}\left(1 - e^{\frac{-2d}{\delta}}\right) = 20\log_{10}\left(1 - 10^{\frac{SE_A}{10}}\right) \quad (5)$$

SE_M mainly depends on the thickness of the material. When the thickness of the shielding layer exceeds the skin depth or when $SE_T > 15$ dB, SE_M can be neglected [72, 73]. However, if the thickness is significantly smaller than the skin depth, multiple reflections must be considered when evaluating the shielding performance.

In addition to macroscopic reflections occurring between the two boundaries of the EMI shielding layer, reflections and scattering can also take place within the microstructure of the shielding material. Such internal multiple reflections and scattering can further extend the propagation path of EM waves, thereby enhancing absorption loss and overall SE.

In summary, SE_R is dominant in highly conductive metallic coatings, SE_A is crucial for magnetic or dielectric loss materials, and SE_M becomes significant only in thin or low-loss multilayer systems where internal reflections cannot be fully attenuated. Understanding the interplay among these terms provides valuable guidance for designing materials with balanced reflection–absorption behavior in EMI shielding applications. It is worth noting that in certain cases, excessive reflection of EM waves may deteriorate the EM environment in the surrounding space. Therefore, researchers have continuously focused on increasing the absorption loss of EMI shielding materials, reducing their reflection loss, and mitigating their environmental impact [74–77].

2.2 Evaluation Criteria

To quantitatively describe the shielding performance, SE is commonly used to evaluate the ability and efficiency of a shielding material in suppressing EMI. SE is influenced by the properties of the shielding material, the frequency of the interference source, the distance between the shielding body and the interference source, as well as various possible discontinuities present in the shield [78, 79]. The SE can be expressed as shown in Eq. (6):

$$SE = 20\log_{10}\left(\frac{E_t}{E_i}\right) = 20\log_{10}\left(\frac{H_t}{H_i}\right) = 20\log_{10}\left(\frac{P_t}{P_i}\right) \quad (6)$$

Here, E_i, E_t, H_i, H_t, P_i, and P_t represent the incident electric field strength, transmitted electric field strength, incident magnetic field strength, transmitted magnetic field strength, incident power, and transmitted power, respectively.

In experiments, EMI SE is typically determined using a vector network analyzer (VNA) by measuring the scattering parameters S_{11} and S_{21}. S_{11} represents the portion of the EM wave emitted from port 1 that is reflected by the shielding material and received again at port 1, while S_{21} represents the portion of the EM wave emitted from port 1 that passes through the shielding material and is received at port

2. Based on Eqs. (7–12), the R, T, A, SE_T, SE_R, and SE_A can be calculated.

$$R = |S_{11}|^2 \tag{7}$$

$$T = |S_{21}|^2 \tag{8}$$

$$A = 1 - R - T \tag{9}$$

$$SE_T = -10\log(T) \tag{10}$$

$$SE_R = -10\log(1 - R) = -10\log\left(1 - |S_{11}|^2\right) \tag{11}$$

$$SE_A = -10\log(T/(1 - R)) = -10\log\left(|S_{21}|^2/(1 - |S_{11}|^2)\right) \tag{12}$$

The functionalization of EMI shielding in fibers is usually achieved through two approaches. One is to deposit conductive layers and magnetic substances on fibers' surface [80–84]. The other is to change the fabric's weaving method from a structural design perspective, altering the transmission direction of EM waves on the fiber surface [85], thereby enhancing the effect of EMI shielding (Fig. 2b). Moreover, in the field of wearable devices, shielding materials are required not only to meet the demands of EMI shielding but also to be "thin" and "light", thereby enhancing the comfort of wearable electronics. In aerospace, integrated circuits, and related fields, lightweight materials can effectively reduce overall weight, saving both energy and space. To evaluate material performance while fully accounting for the effects of thickness and density on SE, we define the following three specific SE parameters (SSE, SE/t, and SSE/t) [86–89]:

$$SSE = \frac{EMI\ SE}{\rho}\left(dB\ cm^3\ g^{-1}\right) \tag{13}$$

$$SE/t = \frac{EMI\ SE}{d}\left(dB\ cm^{-1}\right) \tag{14}$$

$$SSE/t = \frac{EMISE}{\rho \cdot d}\left(dBcm^2g^{-1}\right) \tag{15}$$

The SSE incorporates three key parameters—SE, thickness (d), and density (ρ)—and is particularly important for evaluating the EMI SE of lightweight and thin materials. A higher SSE value indicates that the material is thinner and lighter while still maintaining strong shielding performance. Normalized parameters have been widely applied in the fields of porous EMI shielding materials and ultra-thin EMI shielding materials, especially for multilayer heterogeneous EMI shielding systems. Unlike single-layer materials, multilayer composite materials usually exhibit a synergistic effect due to interface impedance mismatch, multiple internal reflections, and distributed conductive or magnetic loss centers. Therefore, while the absolute SE value reflects the total attenuation capability, SSE provides a weight-normalized shielding efficiency metric, which is crucial for lightweight aerospace and wearable applications. Similarly, SE/t represents thickness-normalized shielding performance and is suitable for ultra-thin coatings and flexible fabrics. The comprehensive index SSE/t further quantifies the shielding per unit mass and thickness.

3 Common Problem and Modification Strategies for High-Performance Inorganic Fiber Materials

Although IHPFs possess superior intrinsic properties, their application in EMI shielding is often hindered by interfacial challenges. Across different fiber systems, one recurring bottleneck emerges—surface inertness. This universal issue governs the extent to which functional coatings or matrix resins can adhere to the fiber surface, directly influencing the integrity and durability of the shielding network. A clear understanding of this common problem is therefore essential before exploring modification strategies to overcome it.

3.1 Common Problem for IHPFs

IHPFs constitute a class of continuous filament materials manufactured via high-temperature melt-drawing or CVD processes from inorganic compounds or elements (e.g., SiO_2, Al_2O_3, SiC, C). Owing to their lightweight nature, exceptional mechanical properties (high specific strength and modulus), outstanding thermal stability, and chemical inertness, they are regarded as ideal structural–functional integrated carriers. These fibers are extensively employed in cutting-edge fields such as aerospace, defense, and industrial infrastructure. Common types include GFs [90, 91], QFs [92], BFs [93–95], CFs [96–98], CNTs fibers [99], graphene fibers [100], and ceramic fibers (e.g., Al_2O_3, BN, SiC, Si_3N_4

© The authors https://doi.org/10.1007/s40820-025-02053-z

fiber) [101–105]. However, their highly stable chemical structures and smooth physical morphologies result in intrinsic surface inertness, which presents common problems for their application in EMI shielding (Table 2). For instance, CFs exhibit a carbon content exceeding 90%, with carbon atoms arranged in a highly ordered structure, leading to pronounced surface inertness [106]. This inertness is primarily manifested as extremely low surface energy and a severe lack of reactive sites, resulting in poor interfacial compatibility and weak physical/chemical adhesion between the fiber surface and functional coatings (e.g., metals, conductive polymers, or carbon nanomaterials). The underlying cause lies in the fact that the intrinsic chemical bonds (e.g., C–C, Si–O, Al–O bonds) of most inorganic fibers (except metallic fibers) are highly stable and covalent, making effective chemical interactions with external substances difficult. This inherent "inertness" can have catastrophic consequences in composite systems; under external stress or thermal cycling, weak interfacial bonding readily becomes the initiation point for failure, causing functional coatings to powder, crack, or delaminate extensively from the fiber surface. Ultimately, this disrupts the EMI shielding network, leading to rapid performance degradation or complete failure. Therefore, effectively overcoming this common challenge through surface activation strategies to establish a robust and durable foundation for subsequent functional coatings is a prerequisite for realizing high-performance and highly reliable fiber-based EMI shielding materials. This section will systematically analyze the nature of this interfacial issue and provide a detailed review of advanced surface treatment strategies to address it.

3.2 Modification Strategies

Addressing the surface inertness of IHPFs not only enables the construction of robust functional layers on the fiber surface, integrating high strength, high modulus, and multifunctionality, but also promotes strong interfaces with various resin matrices, ensuring superior composite performance. Consequently, necessary surface activation pretreatment to increase surface roughness and introduce active chemical groups is a critical prerequisite and the essential first step for constructing durable EMI shielding functional coatings. Based on the phase and medium environment in which the physicochemical processes occur at the fiber interface during treatment, various methods can be categorized into "dry" and "wet" processes (Table 3). It should be noted that the surface modification strategies discussed in this section primarily aim to activate the chemically inert surfaces of IHPFs and improve their interfacial reactivity and adhesion with subsequent coatings or matrices. These activation processes serve as fundamental pretreatments prior to EMI functionalization, while the strategies to construct the EMI shielding functional layers is systematically discussed later in Sect. 4.

3.2.1 "Dry" Surface Modification

Dry processing refers to methods where the fiber surface does not directly contact liquid media (particularly aqueous solutions) during treatment. Reactions or interactions typically occur in gaseous or vacuum environments, such as plasma treatment [107–109], high-energy irradiation [110], ozone treatment [111–113], thermal treatment [114], and vapor deposition [115–117]. Plasma comprises electrons, ions, neutrals, radicals, excited atoms, molecules, and photons, all generated by electron-driven reactions. Plasma surface treatment is highly efficient; its core mechanism involves bombarding the fiber surface with high-energy active species (e.g., oxygen plasma) to introduce polar groups and cause etching. Yang et al. implemented a three-step process of Ar plasma cleaning, O_2 plasma functionalization, and HA plasma polymerization, achieving a synergistic interfacial strengthening effect. After 3 min of treatment, the interfacial shear strength (IFSS) of CF/epoxy composites increased from 39.3 MPa to a maximum of 81.4 MPa (Fig. 3a) [118]. Ozone treatment is another typical dry surface treatment technology. Its core mechanism utilizes the strong oxidizing power of gaseous ozone (O_3) to induce redox reactions on the fiber surface at room temperature, selectively introducing oxygen-containing functional groups and mildly etching the surface, thereby altering the fiber's surface chemical activity and physical structure. Huang et al. subjected pitch-based CFs to ozone treatment, successfully introducing stable oxygen-containing polar functional groups such as carboxyl groups (-COOH), resulting in CFs with enhanced microwave heating performance (Fig. 3b) [119]. Thermal treatment, as an important dry surface treatment technology, can effectively modify the surface chemistry of fibers by controlling the atmosphere and temperature, thereby improving their interfacial

Table 2 Advantages and disadvantages of IHPFs

Advantages	Disadvantages
Ultra-high temperature resistance	High manufacturing cost
High strength-to-weight ratio	Intrinsic brittleness (low strain-to-failure)
Excellent chemical & corrosion resistance	Difficult to cut or machine
Superior creep and fatigue resistance	Limited flexibility
Outstanding thermal stability & low CTE	Poor impact toughness
Electrically/thermally conductive or insulating as desired	Surface inertness → weak fiber-matrix bonding
Tailorable dielectric/EMI shielding properties	Requires specialized sizing or coupling agents
Non-flammable and radiation tolerant	Dense (not lightweight for some ceramic fibers)
Long service life under extreme environments	Limited supply chain & long lead times
Enables multifunctional composites	High processing temperatures (> 1000 °C) for sintering/CVI

compatibility with resin matrices. The core mechanism involves using thermal energy under different atmospheres to selectively remove surface contaminants, introduce or eliminate oxygen-containing functional groups, and modulate the surface microstructure. For instance, Kim et al. systematically studied the effects of thermal treatment in nitrogen (inert atmosphere) and oxygen (reactive atmosphere) on CF properties. The study demonstrated that moderate thermal treatment (300–500 °C) in an oxygen atmosphere is an effective method for enhancing the interfacial activity of CFs through "surface oxidative functionalization", particularly suitable for the surface regeneration and performance recovery of recycled CFs. However, temperature and time must be strictly controlled to avoid degradation of the fiber bulk at excessively high temperatures (Fig. 3c) [120].

Beyond conventional methods such as ozone oxidation and thermal treatment, CVD has emerged as a highly effective surface modification technique for inorganic fibers. By introducing gaseous precursors that undergo chemical reactions on the fiber surface, CVD enables precise control over surface composition and microstructure, thereby significantly enhancing interfacial compatibility with metal matrices and improving electrochemical performance. The core mechanism involves the in situ growth of functional coatings with tailored morphology and chemical properties through careful regulation of reaction temperature, pressure, and precursor types. For instance, Liu et al. employed plasma-enhanced chemical vapor deposition (PECVD) to directly grow vertical graphene (VG) on a GF separator surface using CH_4 as the carbon source at a relatively low synthesis temperature. Subsequent air plasma treatment introduced oxygen and nitrogen heteroatoms, successfully transforming the originally electrochemically inert GF surface into a zinc-affine functional interface. This modification significantly enhanced its affinity toward zinc ions and improved its ability to guide uniform zinc deposition (Fig. 3d) [121].

3.2.2 "Wet" Chemical Modification

"Wet" processing involves treatments conducted in liquid media (typically aqueous solutions, sometimes organic solvents), relying on chemical reactions in the liquid environment to alter the physical and chemical properties of the fiber surface, including liquid-phase oxidation [122], electrochemical oxidation [123], sizing, coating [124], and chemical grafting functionalization [125–127].

Liquid-phase oxidation is a classic "wet" surface modification technique [21]. Its core mechanism leverages the chemical oxidizing power of strong acids (e.g., nitric acid, sulfuric acid) or strong oxidant solutions to efficiently introduce polar functional groups (e.g., oxygen- or nitrogen-containing groups) onto the fiber surface in a liquid environment, while slightly etching the surface to increase specific surface area, thereby significantly improving the fiber's interfacial compatibility and electrochemical activity. Ni et al. achieved a synergistic effect of "functional group introduction" and "pore structure optimization" through liquid-phase oxidation, ultimately endowing nitrogen-doped pitch-based activated CFs (NPACF) with exceptional electrochemical performance in KOH electrolyte. This study demonstrated that liquid-phase oxidation is an efficient, low-temperature, and rapid strategy for fiber surface activation and functionalization, particularly suitable for low-softening-point precursors that cannot withstand high-temperature treatments, providing critical technical support for preparing inorganic high-performance functional fibers (Fig. 4a) [128].

Electrochemical oxidation is an efficient and controllable wet surface treatment technology. Its core mechanism involves using an applied electric field to drive electrochemical reactions of anions (e.g., OH^-, NO_3^-) or water

© The authors https://doi.org/10.1007/s40820-025-02053-z

Table 3 The surface treatment method (to address surface inertness) of IHPFs and the corresponding core mechanism, advantages, and disadvantages

Processing method		Core mechanism	Advantages	Disadvantages	Key parameters	References
"Dry" surface modification	Plasma treatment	Introducing polar groups and etching	High efficiency, environmentally friendly	Time-limited issue, high equipment cost	Flexural strength (109.19 MPa)	[108]
	High-energy irradiation	Breaking surface's molecular chains	High penetration power, no need for vacuum, batch processing	High equipment cost, radiation hazards	IFSS (47.23 → 68.57 MPa)	[110]
	Ozone	Oxidizing and introducing oxygen-containing functional groups	Simple operation, no liquid-phase contamination	Weak oxidation capacity, needing tail gas treatment	MW heating Performance 158 → 203 °C	[119]
	Thermal treatment	Surface lattice reconstruction or generate active surfaces	Simple process, increasing the degree of crystallization	Affecting fibers' mechanical properties, poor controllability	N_2, 1000 °C (tensile strength: 1.26 GPa)	[120]
	Chemical vapor deposition	Gaseous precursors form a solid coating through chemical reactions	High-purity coating, capable of complex shaping	High-temperature damage to fibers, high cost of precursors	1000–1200 °C (deposition); $TiCl_4 \rightarrow Ti$ (H_2)	[116]
"Wet" chemical modification	Liquid-phase oxidation	Strong acids or oxidizing agents erode fiber	Relatively simple, relatively high efficiency	Damage to fibers, heavy contamination	Oxidation time: 10–30 min	[21]
	Electrochemical oxidation	Forming oxygen-containing groups and micro-grooves	Uniform, controllable	High equipment cost	Tensile strength: 65.1 → 94.5 MPa	[23]
	Surface sizing	Coat fibers' surface with a compatible polymer coating	Protect fibers, easy to operate	Limited temperature resistance	IFSS: 9.5 → 20.68 MPa	[27]
	Chemical grafting	Specific functional groups are grafted	Lasting effect, controllable reaction conditions	Grafting ratio, homogeneity	IFSS: 43.6 → 89.6 MPa	[31]

molecules from the electrolyte on the fiber surface, thereby efficiently and uniformly introducing oxygen-containing functional groups and creating nanoscale rough structures, fundamentally enhancing the interfacial bonding performance with resin matrices. For instance, Fu et al. subjected high-modulus CF (HMCF) surfaces to anodic oxidation via electrochemical oxidation treatment, followed by electrochemical grafting of diethylenetriamine. This simultaneously increased the content of oxygen- and nitrogen-containing functional groups on the HMCF surface, significantly improving the interfacial properties of HMCF composites. The interlaminar shear strength (ILSS) of HMCF/epoxy composites reached 97.5 MPa, a 257.1% increase compared to untreated HMCF (Fig. 4b) [129]. Therefore, electrochemical oxidation is considered a highly promising fiber surface activation technology, especially applicable in high-performance composite fields demanding extreme interfacial properties, effectively addressing the interfacial bonding challenges posed by the surface inertness of high-modulus CFs.

Sizing is a "wet" post-treatment technology widely used in industrial production. Its core mechanism involves passing surface-activated fibers through a sizing agent containing polymer film formers, coupling agents, and functional nanoparticles to form a thin, uniform polymer coating on the surface. This coating not only protects the fibers from abrasion but, more crucially, acts as a bridge, generating strong physical adsorption and chemical bonding with both the fiber surface and the resin matrix through its own functional groups, thereby significantly enhancing the composite's interfacial properties. Li et al. innovatively introduced Fe_3O_4 magnetic nanoparticles into a traditional epoxy-based sizing agent. This treatment aimed not only to impart magnetism to BFs but also significantly enhanced their interfacial bonding capacity, fundamentally solving the weak interfacial adhesion caused by the inert surface of BFs. Results showed that both the ILSS and IFSS of the composites were markedly improved after this functional sizing treatment. Additionally, the treatment successfully endowed the fibers and their composites with additional magnetic responsiveness, demonstrating the great potential of sizing technology in achieving integrated "interface strengthening–functionalization" of fibers (Fig. 4c) [130].

Chemical grafting is a "wet" treatment technology that covalently bonds functionally specific molecules or nanomaterials firmly to the fiber surface [131]. It offers strong design flexibility, mild and controllable reaction conditions, and minimal damage to the fiber's mechanical properties. For instance, Ji et al. vertically and uniformly grafted CNTs onto the CF surface by multistep chemical reactions. This structure increased the fiber's specific surface area, providing numerous sites for mechanical anchoring. Furthermore, the grafted CNT network can impart additional functionalities like electrical and thermal conductivity to the composites (Fig. 4d) [132]. Compared to methods like physical coating, chemical grafting via covalent bonds offers durable and stable modification effects that resist debonding under high temperatures or shear forces during processing. It represents one of the most powerful technical pathways for achieving a "qualitative leap" in the interface of fiber composites, particularly suited for cutting-edge applications in aerospace and defense where extreme interfacial performance is required.

4 Preparation Strategies for EMI Shielding Inorganic High-Performance Fibers/Fabrics

IHPFs, owing to their exceptional tensile strength, high modulus, and outstanding environmental resistance, serve as ideal substrates for constructing lightweight and durable EMI shielding materials. However, as previously discussed, their inherent surface chemical inertness and smooth physical morphology severely restrict the robust loading and uniform construction of functional coatings, presenting a primary bottleneck for practical applications. After successfully introducing active sites and improving wettability through surface activation treatments (e.g., plasma, ozone oxidation, and chemical etching), the core research focus shifts to employing precise functionalization strategies to endow these fibers with efficient EMI shielding and absorption capabilities. The key to achieving high-performance EMI shielding lies in constructing a continuous conductive network on the fiber surface and within the bulk phase through precise preparation processes to enhance EM wave reflection loss, while simultaneously introducing abundant magnetic/dielectric loss units, such as metals [133–136], conductive polymers [137–139], carbon-based materials [140–143], and novel materials [144–146] (Fig. 5). This enhances polarization relaxation and energy conversion, thereby promoting the absorption and dissipation of EM waves. To realize this goal, researchers have developed a series of physical and chemical preparation methods (Table 4). Based on

© The authors https://doi.org/10.1007/s40820-025-02053-z

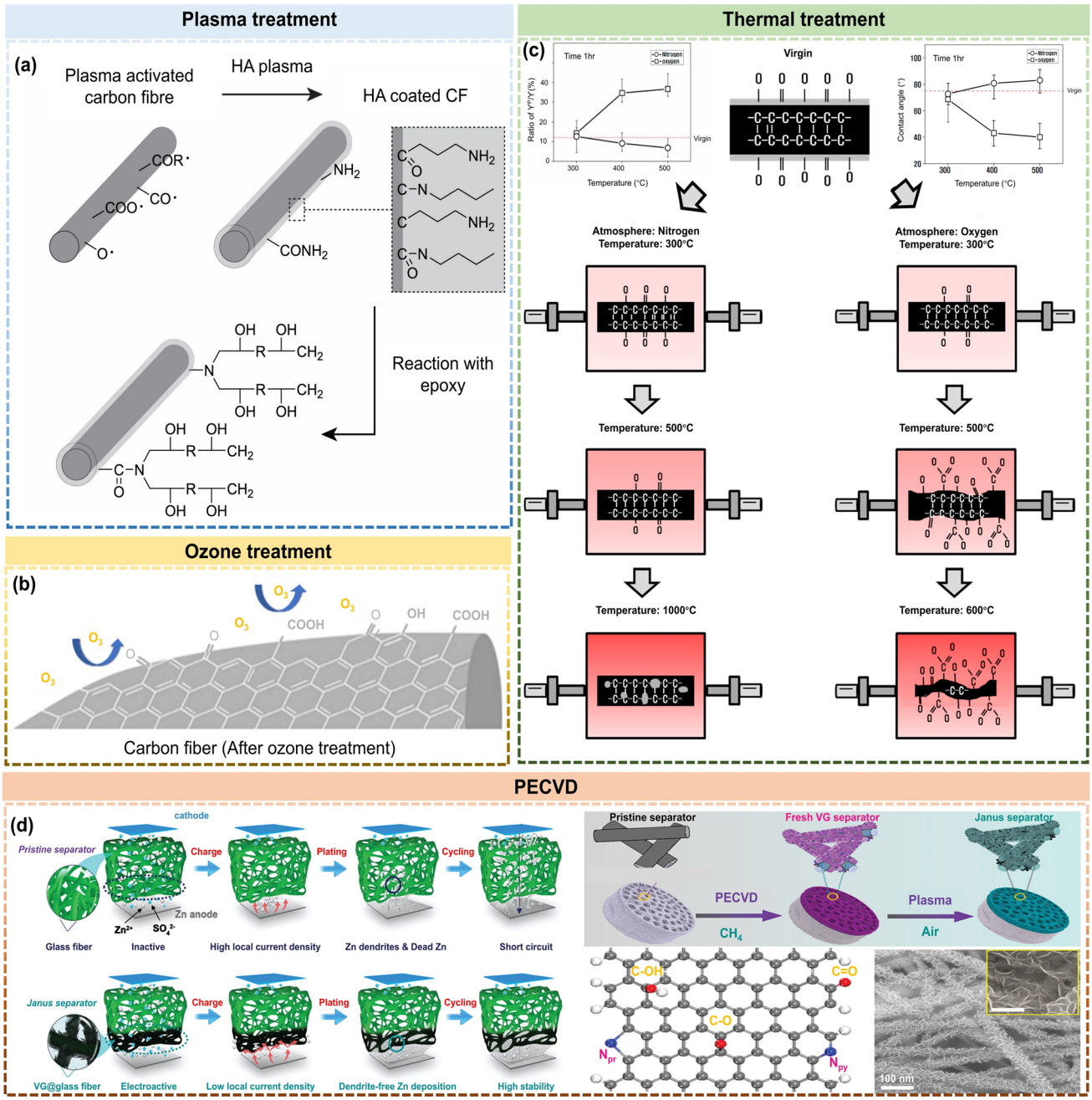

Fig. 3 "Dry" surface modification method for the inert surface of IHPFs: plasma treatment method; ozone; thermal treatment method. **a** HA plasma treatment process and resulting interface with epoxy matrix; The relationship between IFSS, flexural strength (σ_b), and plasma activation-treatment time. Reproduced with permission from [118]. Copyright 2024, Elsevier B.V.; **b** CF's surface after ozone treatment. Reproduced with permission [119]. Copyright 2025, Elsevier B.V.; **c** Surface activity of CFs under different heat treatment environments and temperatures. Reproduced with permission [120]. Copyright 2022, MDPI; **d** Design of Janus separator targeting stabilized Zn anode; Synthetic process of Janus separator; Configuration of O and N-doped graphene. Reproduced with permission [121]. Copyright 2020, John Wiley & Sons

their principles and characteristics, these methods can be primarily categorized into physical deposition, chemical treatment, and other emerging technologies. This section will systematically review the principles and processes of these preparation strategies, delve into how different methods regulate the EM parameters and microstructure of the materials, and ultimately achieve customizable EM

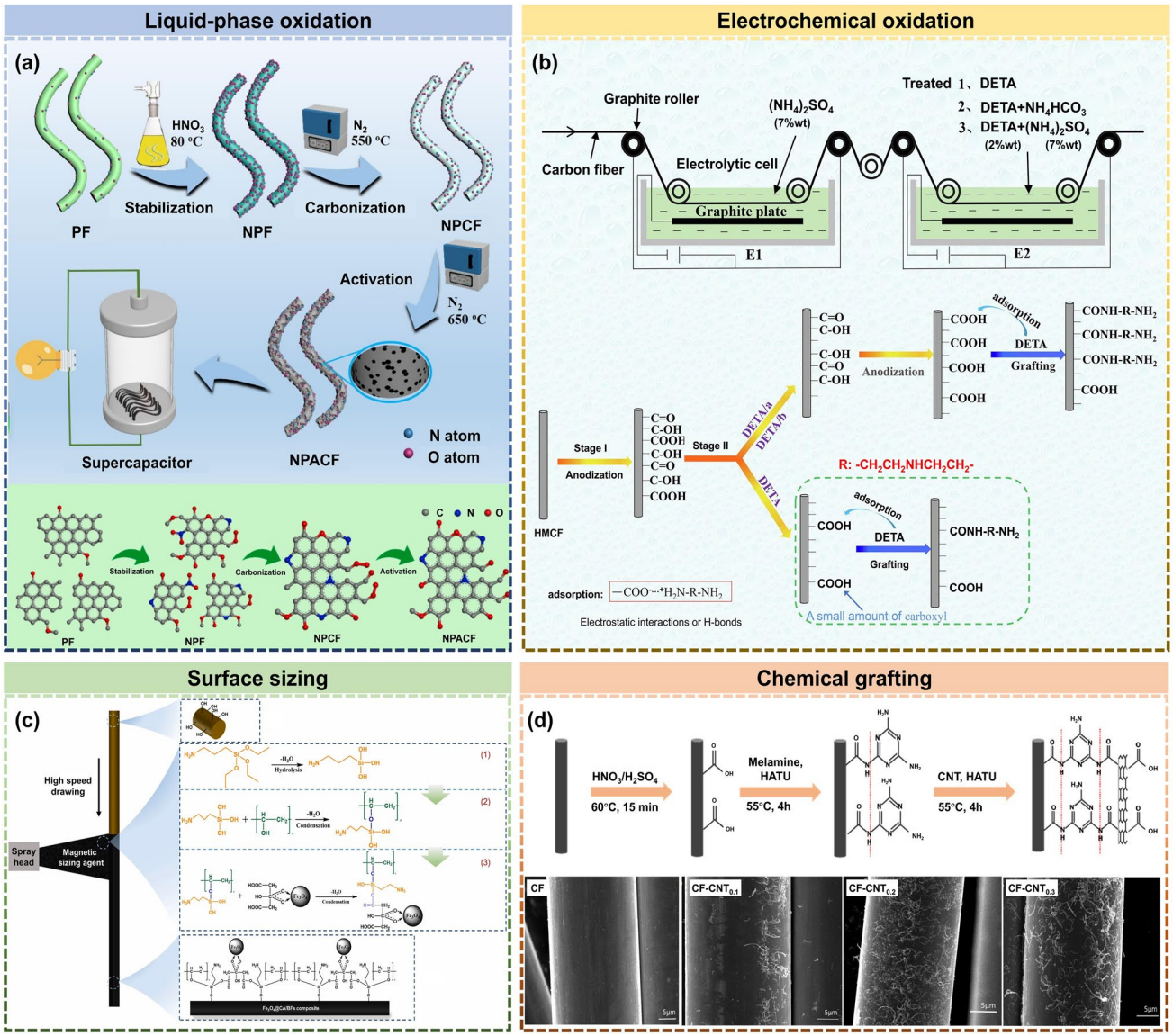

Fig. 4 "Wet" chemical modification method for the inert surface of IHPFs: liquid-phase oxidation; electrochemical oxidation; surface sizing; chemical grafting. **a** Preparation of NPACF; Molecular structural evolution. Reproduced with permission from [128]. Copyright 2024, Elsevier B.V.; **b** Process for electrochemical oxidation-grafting treatment; The reaction mechanism on the surface of HMCF with different treatment methods. Reproduced with permission from [129]. Copyright 2020, Elsevier B.V.; **c** Preparation of BFs, Fe_3O_4@CA magnetic sizing agent and Fe_3O_4@CA/BFs composite. Reproduced with permission from [130]. Copyright 2025, Elsevier B.V.; **d** Chemically grafted modified CFs with CNTs; SEM images of the surface morphologies of CFs. Reproduced with permission from [132]. Copyright 2020, MDPI

protection functions, transitioning from "reflection-dominated" to "absorption-dominated" mechanisms.

4.1 Physical Deposition Method

With the rapid development of electronics in industrial, military, and aerospace sectors, there is a pressing need for adjustable and durable EMI shielding textiles possessing excellent mechanical properties. Physical deposition methods (such as spray-drying, vacuum deposition, and magnetron sputtering) typically involve the physical attachment and film formation of vapor or liquid-phase precursors on the fiber surface. These methods offer advantages including relative process simplicity, minimal damage to the fiber substrate, and ease of scalability [147–149]. Simultaneously, they enable the uniform deposition

© The authors https://doi.org/10.1007/s40820-025-02053-z

of conductive or magnetic material coatings on the fiber surface, significantly enhancing its EMI shielding performance. By adjusting deposition parameters (e.g., deposition rate, atmosphere pressure, and energy input), one can not only optimize the coating's density and adhesion but also impart excellent stability and durability to the fiber fabric. Consequently, physical deposition has become an important and widely applied strategy for modifying IHPFs for EMI shielding.

4.1.1 Spray-Drying

Spray-drying is a relatively mature technology characterized by low cost, simple operation, and high productivity compared to other techniques. These advantages make it particularly suitable for fabricating conductive metal structures on flexible substrates and for large-scale manufacturing [150, 151]. In EMI shielding composite research, multiwalled carbon nanotubes (MWCNTs) [152, 153] and exfoliated graphite nanoplatelets (xGnPs) [154, 155] are widely used to construct efficient conductive networks due to their excellent electrical conductivity and unique micro-morphology, significantly enhancing the material's EMI SE. As shown in Fig. 6a, Park et al. utilized a spray gun to coat a mixed suspension of MWCNTs and xGnPs onto a GF surface, followed by resin infiltration and molding to prepare a multilayer composite shielding material. By optimizing parameters such as MWCNT length, xGnP size, mixing ratio, and number of coating layers, the system enhanced conductive pathways and interfacial structure, ultimately achieving a shielding performance of 35.3–56.8 dB in the frequency range of 30 MHz to 1.5 GHz [156]. The spray-molding process demonstrates good scalability and applicability, laying the foundation for developing multifunctional composites that integrate EMI shielding, self-sensing, and structural intelligence. In the field of EMI shielding composites, AgNWs [157, 158] have become an important material for constructing highly efficient conductive networks due to their high conductivity, large aspect ratio, and excellent mechanical flexibility, making them especially suitable for flexible fabric-based functional composites. As shown in Fig. 6b, Liang et al. modified a GF fabric (GFF) surface with AgNWs via spray-drying and further coated it with a self-cross-linking solid–solid phase change polyethylene glycol (ScPEG) layer based on multiple hydrogen bond cross-linking. The single-layer ScPEG coating A-GFF revealed the excellent and practical function of blocking radio wave transmission of the sample by the change of the indicator light in the safe house. This successfully produced an integrated fabric composite with excellent EMI shielding, thermal management, and information encryption functionalities, offering new ideas for the multiscenario application of high-end EM protection structures in aerospace, military equipment, and smart buildings [159]. Compared to precious metals like silver and gold, copper offers advantages such as lower processing cost, high conductivity, and good ductility, making it a common metallic coating material for enhancing the EMI shielding performance of fiber-based composites [160–162]. Chen et al. used a spray-assisted deposition method to construct a nanostructured copper coating on a CF fabric (CFF) surface. By controlling the number of spraying cycles (10 to 100 cycles), they achieved uniform coverage of a flocculent hierarchical rough structure composed of Cu nanoparticles, which exhibited excellent EMI shielding performance. The SE_T reached approximately 61.3 dB, nearly 20 dB higher than that of untreated CFF. Although the stability of this material under high-temperature and salt spray environments requires further improvement, this study demonstrates the good application potential of spray-assisted deposition technology for preparing lightweight, high-performance flexible EMI shielding textiles [37].

4.1.2 Vacuum Deposition

Vacuum deposition is a physical vapor deposition technique conducted in a vacuum or high vacuum environment, where evaporated or sputtered material is deposited onto the fiber surface. This method effectively reduces interference from gas molecules during the deposition process, resulting in coatings with higher purity and better density [163–165]. By adjusting parameters such as deposition rate, vacuum level, and substrate temperature, the thickness, crystal structure, and adhesion of the coating can be controlled, enabling precise tuning of SE and durability. Furthermore, as this method does not significantly affect the mechanical properties of the fiber, it is considered an effective approach for the surface functionalization of high-performance fibers.

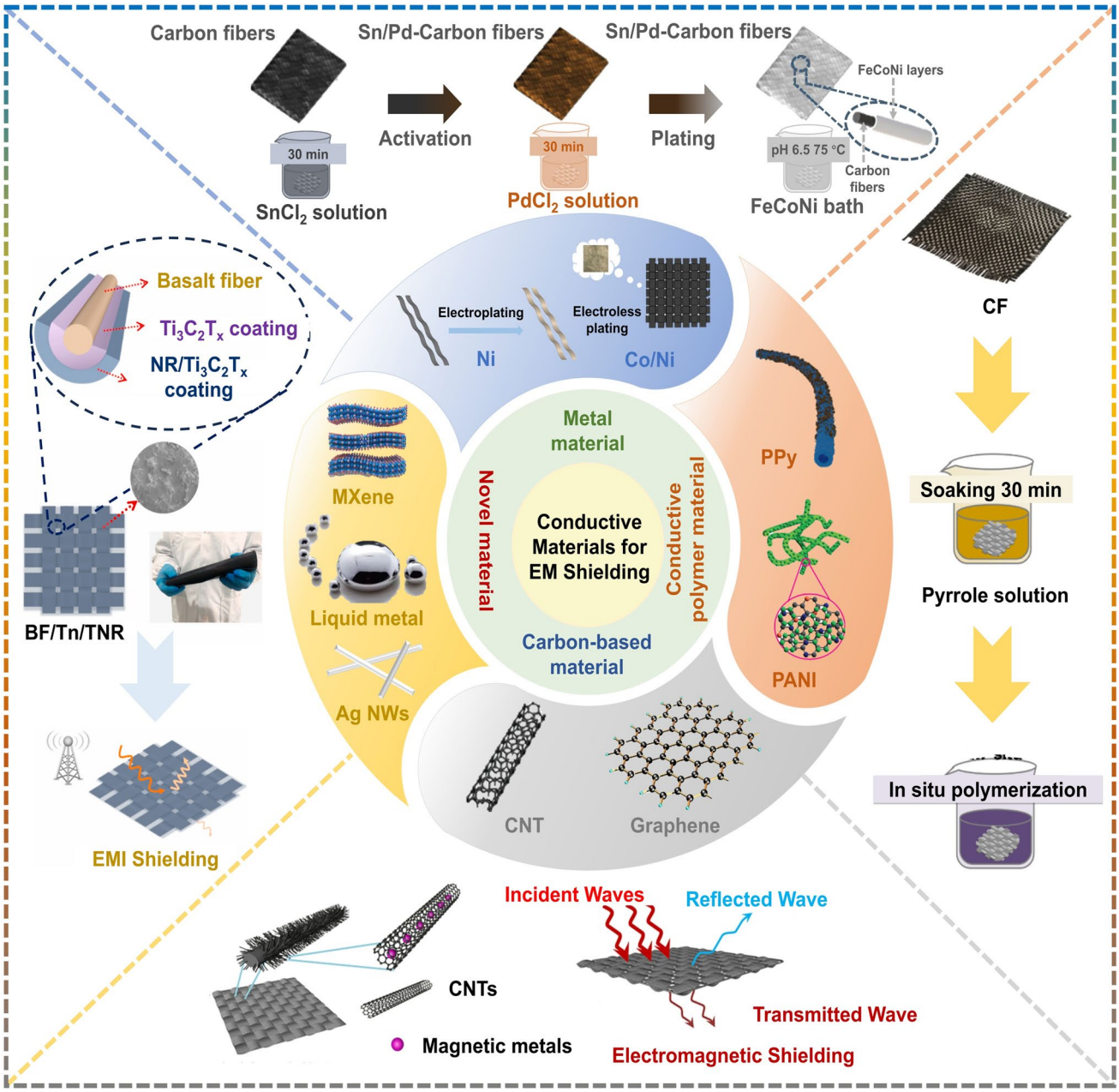

Fig. 5 Conductive materials for constructing the EM shielding functional layer: metals (such as Ni, Co/Ni), conductive polymers (such as PPy, PANI), carbon-based materials (such as CNT, Graphene), new materials (such as MXene, liquid metals (LMs), and AgNWs). Reproduced with permission from: [146] Copyright 2021, Elsevier B.V.; [156] Copyright 2021, MDPI; [177] Copyright 2023, Elsevier B.V

As shown in Fig. 6c, Song et al. used BF as the skeleton, aramid nanofiber (ANF) as the reinforcement, and CNTs as the conductive network. They successfully constructed a BF/ANF/CNT composite paper with a layered structure via vacuum-assisted filtration technology. In the X-band (8.2–12.4 GHz), this material, with a thickness of 48 μm, achieved a SE_T of 24.6 dB. Its SSE per unit thickness (SSE/t) was as high as 12,504 dB cm^2 g^{-1}, demonstrating exceptional EMI shielding performance, environmental stability, and Joule heating performance [166]. The material not only performs excellently under conventional conditions but also maintains structural and functional integrity under extreme conditions, showing broad application prospects. This work provides new ideas for

© The authors https://doi.org/10.1007/s40820-025-02053-z

Table 4 Summary of preparation strategies and key parameters (mechanical property, SSE/t, and other indicators) for the EMI shielding functional layer of IHPFs

Preparation method		Substrate	Materials	Frequency (GHz)	EMI SE (dB)	Temperature	Main cost	Key parameters	References
Physical Deposition	Spray-drying	GF	AgNWs; ScPEG	8–12	40–72	Room temp. (spray)	Materials (precursor); energy for drying	Tensile strength (up to 191 MPa)	[157]
		GF	MWCNT; xGnP	0.03–1.5	35.3–56.8	Room temp. (spray)		Thickness: 3.02 ± 0.03 mm	[154]
		BF	$Ti_3C_2T_x$	8–12	41.53	45 °C (extract); 80 °C (dry)		Electro-thermal property: (4 V, 70 °C)	[144]
		CF	Cu	0.9–1.5	59.8	60 °C (etching)		–	[37]
	Vacuum deposition	CF	CNT	8–12	24.6	50 °C (hot-press)	Equipment; target materials	SSE/t:12,504 dB $cm^2 g^{-1}$	[164]
Chemical treatment	Electroless plating	GF	Cu	8–12	74.59	20–60 °C (deposition); 60 °C (dry)	Materials; wastewater treatment	Cu layer: 8.02 μm	[169]
		GF	Ni; CNTs	8–12; 1–18	> 50; > 35	45 °C (deposition)		CNTs: 9.2 wt%	[168]
		ACBF	Co–Ni alloy	0.03–6	42.57	80 °C (deposition)		Tensile strength (72.9 MPa)	[172]
		CF	Ni-W-Cu-P	8–12	37	75 ± 2 °C (deposition)		Tensile strength (538.8 MPa)	[40]
		CF; Graphene fiber	Ni; Ag	8–12	33.7	Ag: 40 °C, Ni: 60 °C (deposition)		Thickness: 2 mm; Absorption (82.7%)	[167]
	Electroplating	CF	Ni	8–12	71	25 °C (deposition)	Energy; Environmental cost	Thickness: 1.2 mm; Tensile strength (22.4 MPa)	[173]
		CF	Ni	8–12	23.5–31.6	50 °C (deposition)		Flexural strength (21.1% increase)	[43]
		CF–RGO	Ni	2–18	> 10	–		Thickness:2 mm	[42]
	In situ polymerization	CF	PDA, BN	8–12	50.06	60 °C	Equipment; energy; materials	ILSS and mode II toughness (35.50%, 97.35% increase)	[179]
		CoNi/CF	PPy	2–18	68.78	Room temp		EAB: 5.62 GHz; Thickness:2.43 mm	[180]

Table 4 (continued)

Preparation method		Substrate	Materials	Frequency (GHz)	EMI SE (dB)	Temperature	Main cost	Key parameters	References
	CVD	CF	CNT	18–26.5	40–50	900 °C (120 min)	Equipment; energy; materials (precursor gases)	Overpotential: 344 mV	[183]
		BF	CNT	8–12	37.37	800 °C (60 min)		Thickness: 2 mm	[46]
		AF	Graphene	2–18	85	800–1050 °C (1–300 min)		Growth temperature (~200 °C lower); Growth rate (~3.4 times faster)	[185]
		AF	Graphene	2–18	> 30	1100 °C (30–300 min)		CVD flow: CH_4 and H_2	[186]
		AF	Graphene	2–18	46	800–1100 °C (250 min)		CVD flow: C_3H_8 and H_2	[189]
		AF	Graphene	8–12	25	1000 °C (30 min)		Absorption: > 90%	[117]
	Thermal treatment	Graphene fiber	–	8–12	> 120 (2L)	600–2800 °C (60 min)	Equipment; energy; heating time; gas purity	8.5×10^5 S m^{-1}	[191]
		CF	CNT (ZIF–8@ZIF–67)	2–18	> 20	920 °C (pyrolysis)		EAB: 4.4 GHz; Thickness: 1.38 mm	[192]
		CF	CNT(ZIF-L)	8–12	38.4	400 °C (2 h); 900 °C (6 h)		7.50 W m^{-1} K^{-1}	[193]
Others	ALD	CF	$Al_2O_3 + TiO_2$ layers	8–12	45	150 °C	Equipment; materials (precursor)	Structure color	[198]
	Laser etching	BF	Graphene	8–12	~20 (1 L); ~50 (3 L)	Localized high temp	Materials; safety management	–	[200]
	Dipping	CF	MWCNT	2; 2.7	37; 68	Room temp	Materials	SSE/t: 35,000 dB cm^2 g^{-1}	[203]

addressing the reliability issues of EMI shielding materials in extreme environments and offers important references for the design and preparation of multifunctional integrated flexible electronic materials.

4.2 Chemical Treatment Method

Compared to physical deposition methods, chemical treatment techniques construct functional coatings on fiber surfaces through chemical reactions or modulation of the chemical environment, offering advantages such as strong adhesion, continuous film formation, and multiscale interfacial control. Typical methods include electroless plating, electroplating, in situ polymerization, chemical vapor

© The authors https://doi.org/10.1007/s40820-025-02053-z

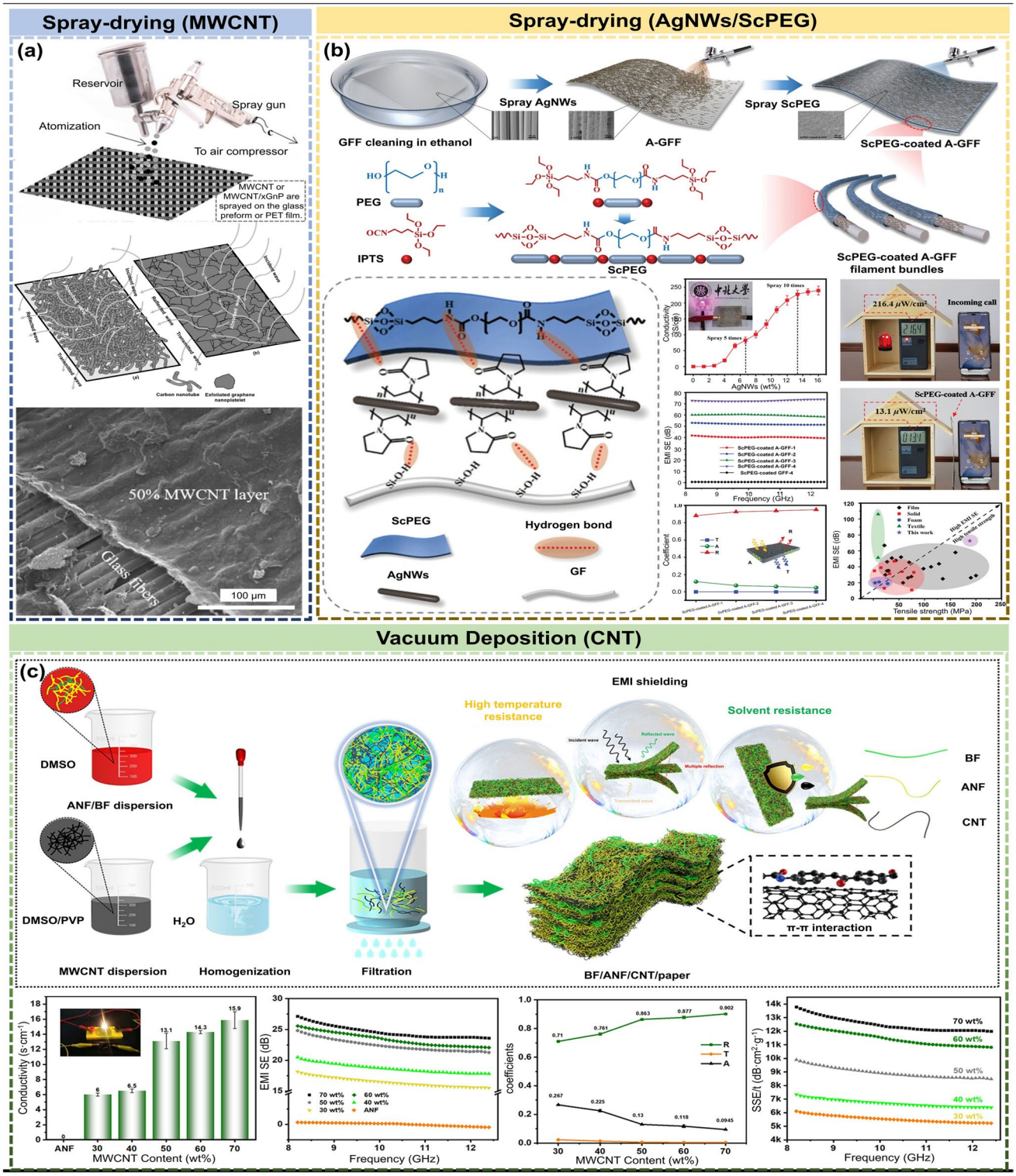

Fig. 6 Physical deposition method: spray-drying and vacuum deposition, are used to fabricate EMI shielding functional layers. **a** MWCNT or MWCNT/xGnP are sprayed on the GFs; Illustration of EM waves interactions with CNTs and xGnPs; SEM micrographs of hybrid MWCNT/xGnP coated GFs. Reproduced with permission from [156]. Copyright 2019, Elsevier B.V.; **b** Fabrication of the ScPEG-coated A-GFF; Hydrogen bonds among ScPEG coatings, silver nanowires (AgNWs), and fabric; The conductivity as a function of AgNWs content with different spraying times; EMI SE and power coefficient of ScPEG-coated A-GFF; EMI shielding mechanism. Reproduced with permission from [159]. Copyright 2024, Elsevier B.V.; **c** Fabrication process of BF/ANF/CNT composite paper; Electrical conductivity, EMI SE, power coefficient, and SSE/t of BF/ANF/CNT composite paper. Reproduced with permission from [166]. Copyright 2023, John Wiley & Sons

deposition/infiltration, and annealing treatments. Chemical treatments can introduce highly conductive or magnetic functional layers onto the fiber surface, while effectively regulating coating thickness, microstructure, and interfacial adhesion by adjusting reaction conditions (e.g., solution concentration, temperature, reaction time, and catalyst type) [167]. These methods not only endow IHPFs with excellent EMI SE but also balance flexibility, durability, and stability in complex environments, thereby holding broad application potential in the preparation of EMI shielding fiber composites.

4.2.1 Electroless Plating

Electroless plating is an autocatalytic reduction process that does not require an external power source, enabling the uniform deposition of conductive metal layers on fiber surfaces [168, 169]. Its advantage lies in achieving continuous coverage on fibers or fabrics with complex morphologies, with coating thickness controllable via reaction time and solution composition. Commonly used metals include Ni, Cu, and Ag, which significantly enhance the electrical conductivity and EMI shielding performance of fibers [170–172]. Simultaneously, the coatings formed by electroless plating exhibit strong adhesion to the substrate, imparting excellent durability and stability to the fibers, making this method widely applicable in the construction of EMI shielding textiles. Copper electroless plating, due to its mature technology, low cost, and ease of scalability, is extensively used to build continuous metallic conductive layers on fiber surfaces, particularly for the EMI shielding functionalization of IHPFs like GFs. As shown in Fig. 7a, Parkash et al. achieved continuous and dense copper layer coverage on the inert surface of GFs via electroless copper plating, with a SE_T of 74.59 dB in the X-band, significantly superior to that of untreated GFF ($SE_T = 1.10$ dB). They systematically investigated the effect of deposition temperature (20–60 °C) on the microstructure, electrical conductivity, and EMI shielding performance of the electroless copper layer on GFF [173]. By precisely controlling the deposition temperature, the crystallinity, thickness, and density of the copper layer could be regulated, enabling the production of high-performance, lightweight, and flexible EMI shielding textiles without complex pretreatment.

Beyond single-metal coatings, alloy electroless plating also demonstrates significant advantages in enhancing the EMI shielding performance of fiber-based composites due to its tunable multifunctional properties [174, 175]. Wang et al. successfully constructed a cobalt–nickel (Co–Ni) alloy coating on the surface of an aramid-carbon blended fabric (ACBF) using electroless plating, markedly improving the material's EMI SE and mechanical strength. The average SE_T reached 42.57 dB in the 30–6000 MHz frequency range, primarily attributed to the synergistic effect between the dielectric loss of CFs and the magnetic loss of the Co–Ni alloy, achieving dual attenuation of EM wave absorption and reflection. Furthermore, the material exhibited excellent corrosion resistance and high mechanical strength, showing broad application prospects in fields such as aerospace flexible electronic equipment and military protective textiles (Fig. 7b) [176]. This method features a mild process that avoids strong acids or alkalis and can be completed within 2–3 h, demonstrating good potential for industrialization. Electroless coatings endow IHPFs with high conductivity, forming continuous conductive networks responsible for reflection-dominated EMI shielding. In addition, the in situ redox deposition process facilitates strong chemical bonding between the coating and the fiber surface, significantly enhancing interfacial adhesion and mechanical integrity.

4.2.2 Electroplating

Electroplating is a method that uses an external electric field to drive the reduction and deposition of metal ions onto fiber surfaces, enabling the acquisition of highly dense and pure metal coatings in a relatively short time. Compared to electroless plating, electroplating offers higher controllability over deposition rate and thickness and is suitable for large-area continuous processing. By adjusting process parameters such as current density, electrolyte concentration, and temperature, the adhesion and microstructure of the coating can be effectively improved, thereby enhancing EMI shielding efficiency. However, electroplating typically requires the fiber substrate to possess some conductivity, so it is often combined with other surface activation or pretreatment methods. As shown in Fig. 7c, Wang et al. used electroplating to construct two types of nickel coatings on CF surfaces: conventional flat and nanocone-shaped (denoted as CF@

© The authors https://doi.org/10.1007/s40820-025-02053-z

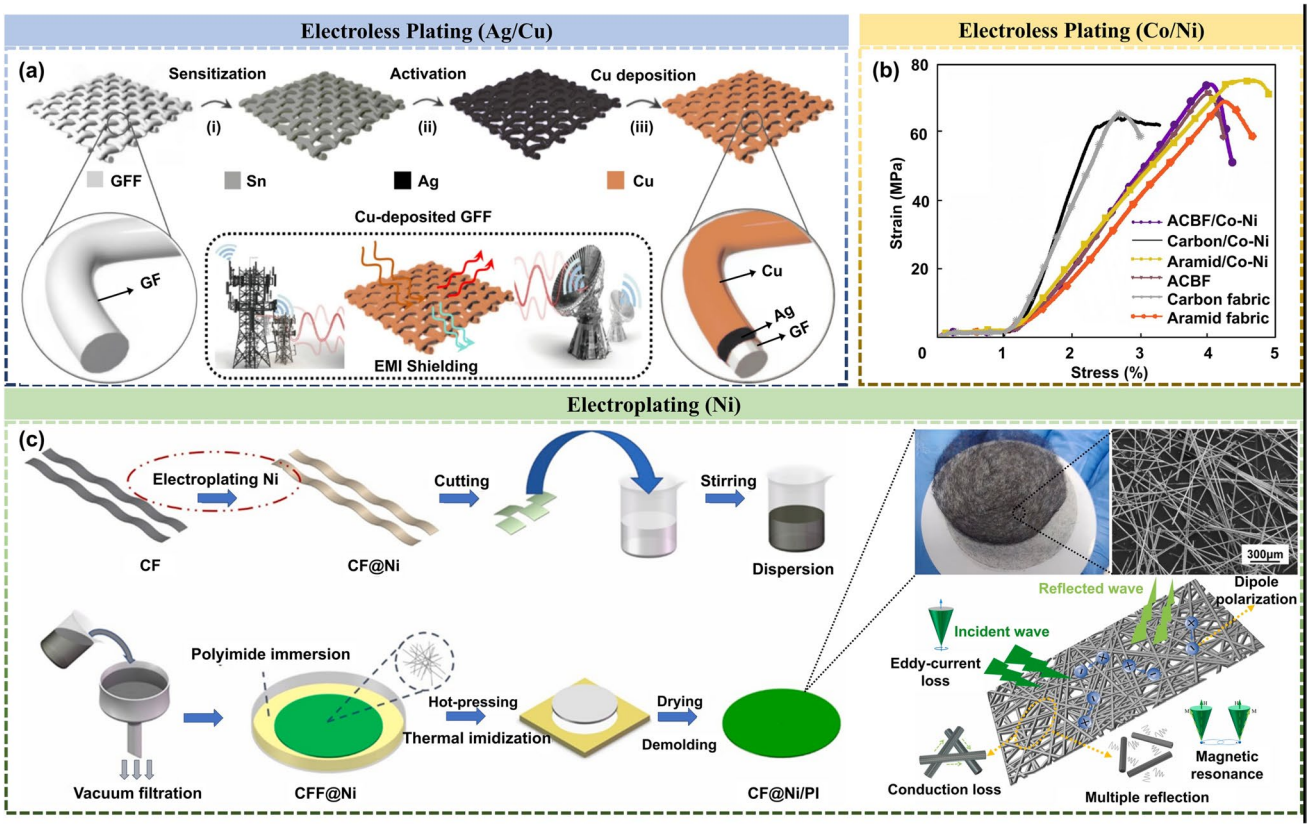

Fig. 7 Fabrication for EMI shielding functional layers by electroless plating and electroplating method. **a** Fabrication process for electroless Cu deposition on GFF. Reproduced with permission from [173]. Copyright 2025, Elsevier B.V.; **b** Stress–strain curves of ACBF/Co–Ni and other samples (The intrinsic toughness of Co–Ni alloy coating enhances the tensile strength of ACBF/Co–Ni.). Reproduced with permission from [176]. Copyright 2021, Elsevier B.V.; **c** Fabrication process of the proposed composite film; Optical and SEM images of CFF@Ni; EM shielding behavior of CF@NN/PI. Reproduced with permission from [177]. Copyright 2023, Elsevier B.V

CN and CF@NN, respectively). They found that differential adsorption of NH_4^+ ions in the plating solution induced the growth of nickel grains along specific orientations, forming nanocone array structures approximately several hundred nanometers in height (CF@NN). This structure not only enhanced the contact probability and mechanical interlocking effect between fibers but also significantly improved the electrical conductivity (41.2 S m^{-1}) and EMI SE_T (71 dB in the X-band at a thickness of only 1.2 mm) of the composite film. Additionally, the CF@NN/PI composite film exhibited excellent mechanical properties (tensile strength of 22.4 MPa, elastic modulus of 90 MPa) and flexibility, withstanding repeated bending without fracture, indicating broad application prospects in microelectronic devices and flexible wearable systems [177].

4.2.3 In Situ Polymerization

In situ polymerization refers to the method of directly initiating monomer polymerization reactions on the surface of fibers or fabrics to form conductive polymer coatings. Common polymers include polypyrrole (PPy) [178], polyaniline (PANI) [179], and polythiophene (PTh) [180]. These conductive polymers not only impart excellent electrical conductivity to fibers but also combine lightweight, flexibility, and good processability. By controlling polymerization conditions (e.g., type of oxidant, reaction temperature, and monomer concentration), the coating thickness, conductivity, and interfacial adhesion can be regulated controllably, making this a strategy that balances performance and process applicability in EMI shielding fibers. It is particularly suitable for constructing polymer coatings that integrate conductivity, dielectric properties, and

good interfacial bonding [181, 182]. As shown in Fig. 8a, Luo et al. successfully constructed a core–shell structured boron nitride/short CF (BN/SCF) on the surface of SCF via polydopamine (PDA)-assisted in situ polymerization and electrostatic assembly technology. Using high-voltage electrostatic flocking to achieve oriented alignment, they ultimately prepared a multifunctional CF/epoxy composite via vacuum-assisted resin infusion (VARI). The composite achieved an EMI SE of 50.06 dB, while the ILSS and fracture toughness increased by 35.50% and 97.35%, respectively, providing a new approach for realizing lightweight, high-shielding, and tough integrated composites through in situ polymerization interface engineering [183].

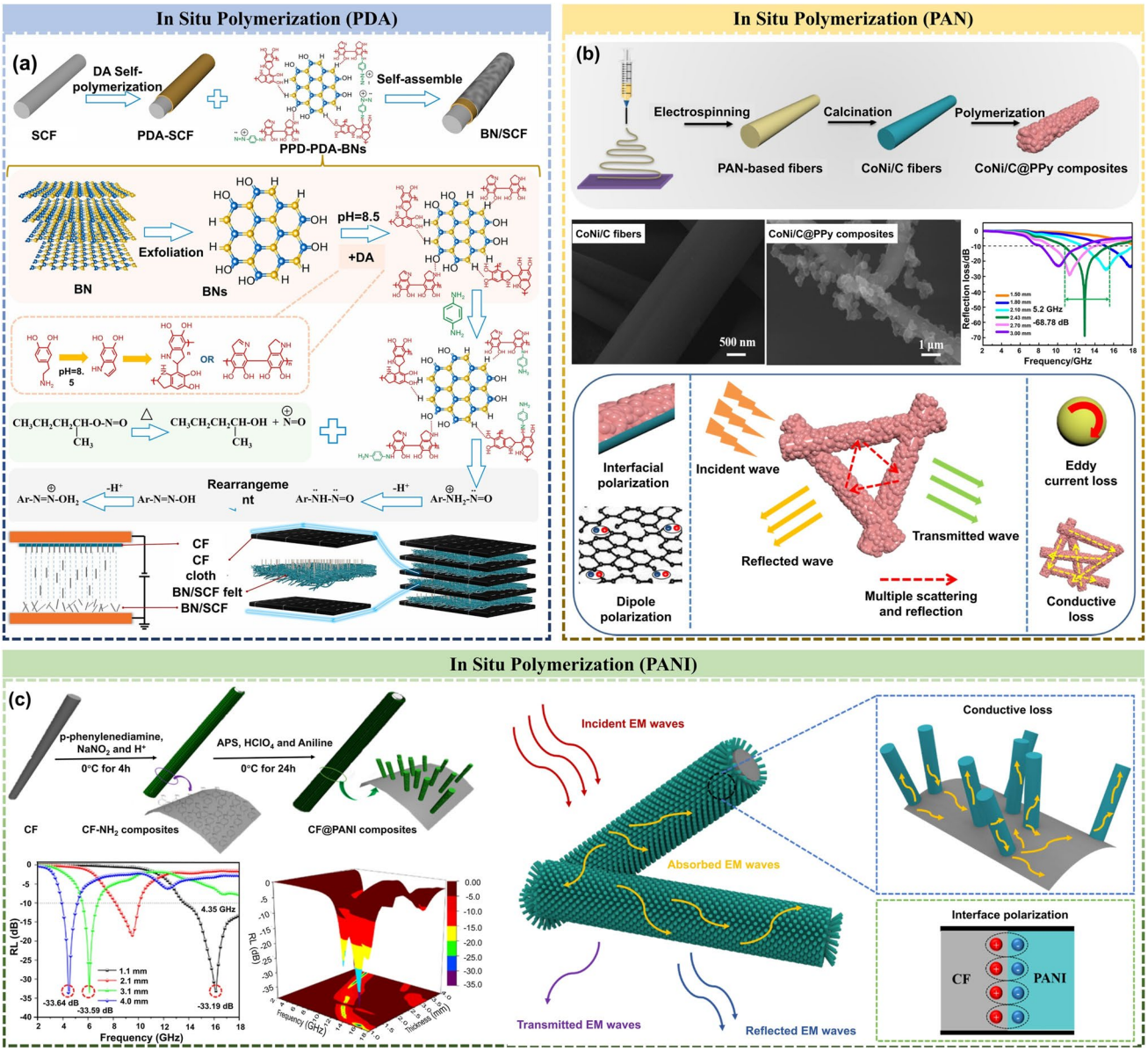

Fig. 8 Fabrication for EMI shielding functional layers by in situ polymerization method. **a** Preparation of BN/SCF; Preparation of PPD-PDA-BNs; Preparation of BN/SCF felt-x/CF/EP composites. Reproduced with permission from [183]. Copyright 2025, Elsevier B.V.; **b** Synthesis processes of CoNi/C@PPy composites; SEM images of CoNi/C fibers and CoNi/C@PPy composites; RL values of CoNi/C; The possible EM wave absorption mechanisms of CoNi/C@PPy composites. Reproduced with permission from [184]. Copyright 2022, Elsevier B.V.; **c** Synthesis procedure of CF@PANI; RL and 3D plots of CF@PANI composites; EM wave-absorbing mechanisms. Reproduced with permission from [185]. Copyright 2025, Elsevier B.V

© The authors https://doi.org/10.1007/s40820-025-02053-z

Besides PDA, PPy is another commonly used conductive polymer widely applied in the functional modification of fiber surfaces to enhance their EMI performance. As shown in Fig. 8b, Ma et al. prepared CoNi alloy-embedded CFs (CoNi/C) via electrospinning and carbonization technology, and further coated them with PPy using in situ polymerization to successfully construct CoNi/C@PPy composites. The material exhibited excellent EM wave absorption performance from low frequency to the Ku band, with a minimum reflection loss (RL_{min}) of –68.78 dB and an effective absorption bandwidth (EAB) of 5.2 GHz, achieved at a low filler loading of only 15 wt% [184]. Research indicated that the introduction of PPy not only enhanced the conductive loss and interfacial polarization of the material but also significantly optimized impedance matching and attenuation capability through its synergistic effect with CFs and magnetic particles. Furthermore, Gou et al. constructed a core–shell structured CF@PANI composite functional layer by covalently grafting polyaniline nanorods (PANI) onto amino-functionalized CFs ($CF-NH_2$) via diazonium reaction and in situ polymerization (Fig. 8c) [185]. The CF@PANI–5 sample exhibited optimal EM wave attenuation capability. Compared with CVD and other vapor-phase deposition techniques, in situ polymerization does not require high-temperature treatment. The resulting polymer layer has moderate electrical conductivity and inherent flexibility. It can not only prevent micro-cracks in the bottom coating during material bending or thermal cycling, but also is suitable for combining with other technologies to construct EMI shielding functional layers that combine reflection and absorption. Looking to the future, optimizing the interfacial chemistry between the polymer and the fiber, the developing green, scalable polymerization methods will be the key to advancing flexible and sustainable EMI shielding materials.

4.2.4 Chemical Vapor Deposition

CVD is a method that utilizes gaseous precursors which decompose at high temperatures and deposit onto fiber surfaces. This technique can form inorganic coatings—such as carbon, carbides, or metal oxides—that are structurally dense, uniformly thick, and tightly bonded to the substrate [186–188]. CVD demonstrates outstanding performance in enhancing the thermal stability, corrosion resistance, and EMI shielding properties of fibers. As shown in Fig. 9a, Liu et al. directly grew graphene on the surface of alumina fiber fabric (AFF) using a self-designed roll-to-roll CVD system, successfully preparing graphene-coated alumina fiber fabric (GAFF). The study, for the first time on a non-metallic substrate, revealed a metal-catalysis-like "vapor-surface–solid" (VSS) growth mechanism. Compared to the traditional "vapor–solid" (VS) model followed on conventional non-catalytic non-metallic substrates; this mechanism significantly reduced the graphene growth temperature (by approximately 200 °C) and increased the growth rate (by about 3.4 times). The obtained GAFF not only inherited the high strength, lightweight, and flexibility of the alumina fibers but also exhibited broadly tunable electrical conductivity and excellent EMI shielding performance (SE_T up to 85 dB). Furthermore, the self-designed roll-to-roll CVD system enabled the stable large-scale production of GAFF, laying a solid foundation for its practical application in efficient, lightweight EMI shielding composites [189]. Building on this research, Liu et al. further explored the potential of GAFF for multifunctional integration and broad-spectrum performance regulation. By precisely controlling the thickness of the graphene during CVD and the pore structure of the fabric itself, they successfully achieved wide-range adjustment of multiple performance parameters of GAFF, including electrical conductivity, electrothermal temperature, and EM wave reflectivity and transmissivity. This not only enabled the roll-to-roll mass production of GAFF in multiple specifications but also promoted the leapfrog development of graphite-based composites from single function to multidimensional compatibility of "structure–function–environment" (Fig. 9b) [190].

Methane (CH_4) is commonly used as a carbon source for graphene growth on insulating substrates [191, 192]. Based on their previous work, Liu et al. further explored the feasibility of using propane (C_3H_8) for the rapid preparation of graphene on AFF and systematically compared its growth behavior and mechanism with traditional carbon sources (CH_4, C_2H_4). The study found that C_3H_8 pyrolysis at high temperatures generates unique active carbon species, C_3H, which exhibit lower migration energy barriers, higher nucleation density, and faster growth rates on the AFF surface, thereby significantly enhancing the coverage speed and quality of graphene. Compared to CH_4 and C_2H_4, C_3H_8 reduced the nucleation time from 110 and 48 min to just 2 min, increased the nucleation density by 160 and 50 times, respectively, and increased the growth rate by more than 10

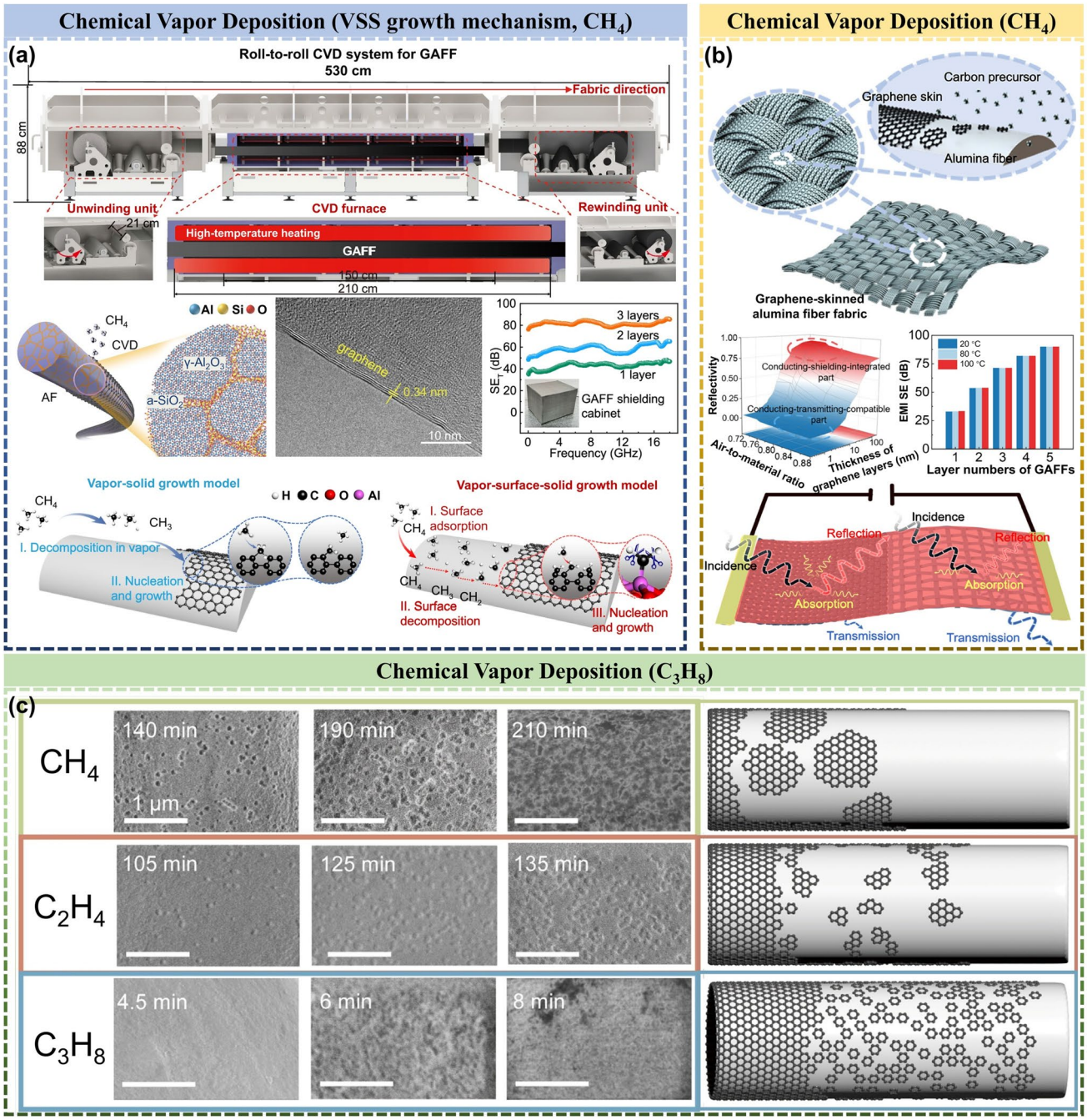

Fig. 9 Fabrication for EMI shielding functional layers by CVD method. **a** Mass production of GAFF with the home-made roll-to-roll CVD growth; High resolution-transmission electron microscope (HRTEM) image of three-layer graphene on AF; EMI SE of GAFF; Graphene vapor–solid growth model and graphene vapor surface–solid growth model. Reproduced with permission from [189]. Copyright 2025, John Wiley & Sons.; **b** Preparation of GAFFs via CVD process; EM reflectivity of GAFFs with different air-to-material ratios and graphene coating thicknesses; Adjustable electrothermal-electromagnetic-compatible performances. Reproduced with permission from [190]. Copyright 2025, John Wiley & Sons. **c** SEM images of the graphene domain regions on AF with three carbon sources of CH_4, C_2H_4, and C_3H_8; Comparison of the graphene growth behavior of C_3H_8, CH_4, and C_2H_4 carbon sources. Reproduced with permission from [193]. Copyright 2025, Tsinghua University Press Ltd

© The authors https://doi.org/10.1007/s40820-025-02053-z

times, achieving near-complete coverage efficiently within 8 min. The resulting GAFF not only possessed excellent tunable electrical conductivity, high mechanical strength, and flexibility but also showed broad application prospects in EMI shielding (Fig. 9c) [193]. This research provides a new strategy for the efficient, large-area, transfer-free preparation of graphene on non-catalytic insulating substrates, advancing the practical application of graphene in functional composites. Furthermore, for CVD technology, the composition and microstructure of the coating can be precisely regulated by optimizing the reaction atmosphere, temperature, and precursor types, forming carbon nanostructures with hierarchical conductive networks, thereby triggering multiple scattering, dielectric polarization and conductive loss, achieving EMI shielding through both reflection and absorption. The in situ growth process ensures excellent interface contact between the carbon coating and the fiber substrate, forming conductive pathways with excellent interface adhesion and thermal stability. However, the high processing temperature and equipment cost of CVD are still obstacles for large-scale implementation. Future work can focus on improving methods such as low-temperature catalytic growth to achieve a broadband, efficient and scalable EMI shielding system.

4.2.5 Thermal Treatment

Thermal treatment is typically employed as a post-processing step following chemical deposition to improve the structure and properties of metal or inorganic coatings. At high temperatures, grains within the deposited layer grow, while defects and interfaces are reduced, thereby enhancing the density and electrical conductivity of the coating. For metal-plated fibers, annealing not only strengthens the adhesion between the coating and the substrate but also reduces interfacial stress, improving its stability and durability [194]. The choice of annealing temperature and time significantly influences the coating's microstructure and EMI SE; therefore, an appropriate heat treatment process is crucial for achieving high-performance EMI shielding fibers.

Furthermore, beyond the strategy of directly growing graphene on substrate surfaces, high-temperature annealing of preformed carbon-based fibers has also emerged as a key method for optimizing their intrinsic electrical and EM properties. As shown in Fig. 10a, Gao et al. prepared graphene oxide (GO) fibers via wet spinning and obtained a series of graphene fibers through chemical reduction and high-temperature annealing (600–2800 °C). The heat treatment optimized the structure and significantly enhanced the electrical conductivity of the fibers, increasing from 1.2×10^4 S m^{-1} after chemical reduction to 8.5×10^5 S m^{-1} after annealing at 2800 °C. When woven into fabric, it exhibited exceptional EMI shielding performance in the X-band: the SE_T of a single-layer fabric reached up to 96 dB, and by adjusting the texture direction and layering, the SE_T of up to 126 dB could be achieved, along with excellent flexibility and durability [195]. This work demonstrates that high-temperature heat treatment is an efficient and scalable strategy for repairing the structure of carbon materials and enhancing their intrinsic shielding performance, providing an important pathway for developing next-generation high-performance flexible EMI shielding textiles.

While directly optimizing the intrinsic conductive and shielding properties of carbon-based fibers through high-temperature heat treatment, another strategy based on the thermal conversion of metal–organic frameworks (MOFs) to derive CNTs offers a new approach for constructing hierarchical structures and achieving efficient, green EMI shielding. Hou et al. developed a novel method for the selective growth of CNT cluster arrays on the CF surface. This method used PS microspheres as a mask to regulate the distribution of surface functional groups on CF. Through bimetallic ZIF-8@ZIF-67 MOF coating and subsequent high-temperature pyrolysis, Co-doped CNT cluster arrays were catalytically grown in specific regions (Fig. 10b) [196]. Research indicated that the density and distribution of the CNT clusters could be precisely controlled by the concentration of PS microspheres and the degree of H_2O_2 treatment. In terms of EMI shielding performance, the material's SE_T exceeded 20 dB in the 2–18 GHz range, with a maximum green shielding index (g_s) of 351 and $g_s > 12$ across the entire frequency band, far superior to the commercial green shielding standard ($g_s > 1$), demonstrating excellent absorption-dominated green shielding characteristics. Moreover, extending this method to integrated thermal management-EMI shielding composites enables multifunctional synergy and performance enhancement. Wu et al. achieved in situ growth of leaf-like bimetallic ZIF-L (Co/Zn) on the surface of CF cloth (CFC) followed by high-temperature conversion, successfully constructing a three-dimensional interconnected network of aligned CFs bridged by carbon

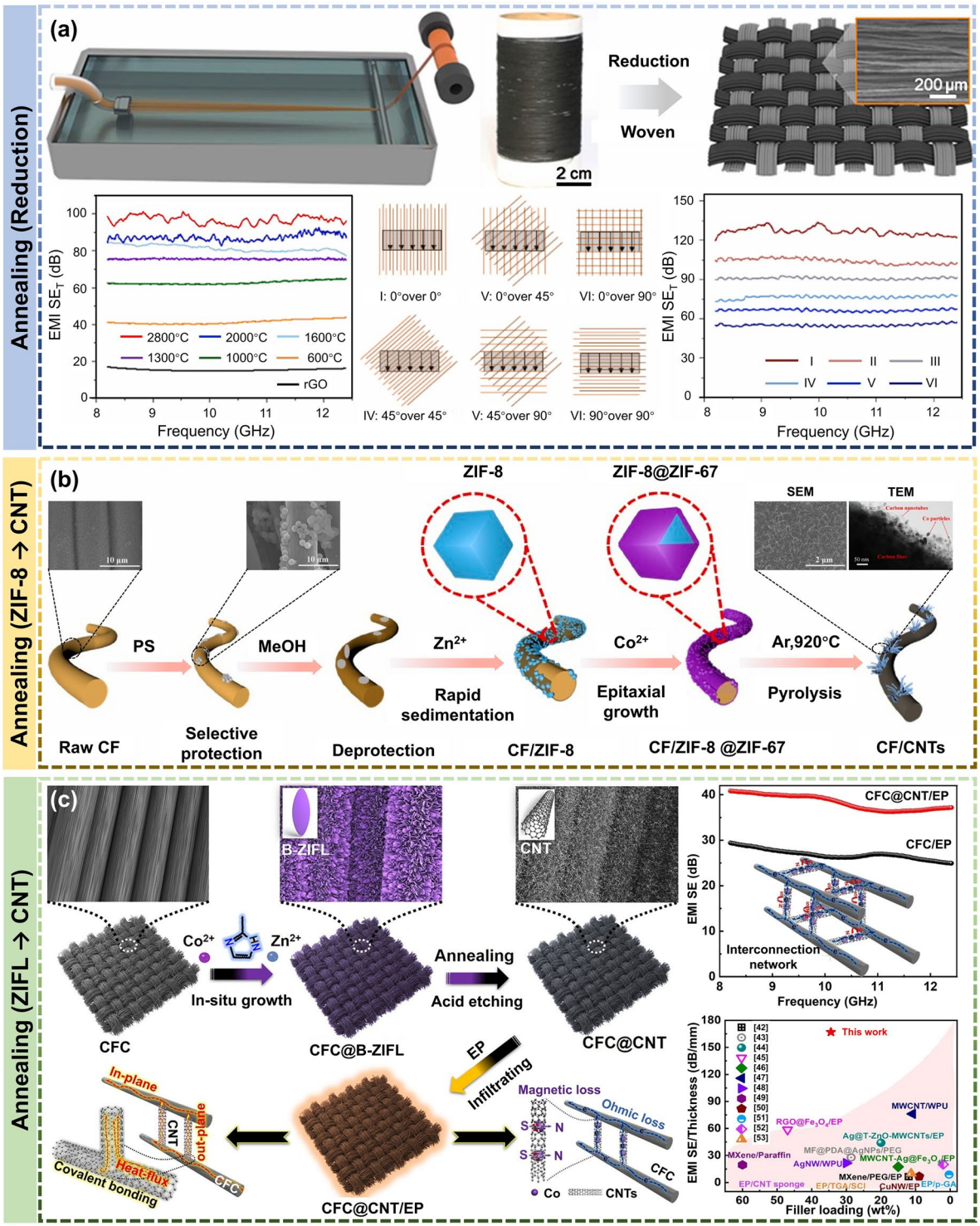

Fig. 10 Fabrication for EMI shielding functional layers by thermal treatment method. **a** Preparation and EMI SE of graphene fiber fabrics, and combinations of overlapping two layers of graphene fiber fabrics. Reproduced with permission from [195]. Copyright 2024, Elsevier B.V.; **b** Growth process of CNT cluster arrays on CF (ZIF-8@ZIF-67 transforms into CNTs by pyrolysis). Reproduced with permission from [196]. Copyright 2023, Elsevier B.V.; **c** Synthesis process, isotropic heat transfer, and EMI shielding behavior of CFC@CNT/EP (EMI shielding performance of CFC@CNT/EP is significantly superior to that of existing studies.). Reproduced with permission from [197]. Copyright 2022, American Chemical Society

© The authors https://doi.org/10.1007/s40820-025-02053-z

nanotubes (CFC@CNT). This was further compounded with epoxy resin (EP) to create a multifunctional composite. In this structure, the ZIF-L-derived CNTs not only effectively connected adjacent CFs, significantly reducing interfacial thermal resistance, but the encapsulated Co nanoparticles also provided stable magnetic loss capability. The resulting CFC@CNT/EP composite exhibits exceptional anisotropic thermal conductivity and high-efficiency EMI SE (38.4 dB). Furthermore, the composite maintains stable mechanical properties, thermal conductivity, and shielding performance even after hundreds of bending cycles, demonstrating outstanding comprehensive application potential (Fig. 10c) [197]. Thermal treatment plays a crucial role in the crystallinity, phase composition, and interface microstructure of each functional layer on IHPFs. Appropriate annealing not only enhances the electrical and magnetic properties of the coating (NiO → Ni) by promoting grain growth and defect repair, thereby regulating the two dominant EMI shielding mechanisms of reflection and absorption, but also improves the interface diffusion and adhesion between the coating and the fiber substrate. However, excessively high temperatures may damage the integrity of the fibers or cause the coating to crack. Therefore, optimizing the thermal treatment scheme and environmental control is crucial for achieving a balance between the material's electrical conductivity and mechanical stability.

4.3 Other and Emerging Technologies

Beyond traditional physical deposition and chemical treatment methods, several emerging technologies have gradually been applied to the surface functionalization of IHPFs in recent years. Novel techniques such as ALD and laser etching, leveraging their atomic-level processing precision or unique structural design capabilities, are paving new ways for the design of next-generation intelligent and ultra-efficient EMI shielding materials. Compared to conventional processes, these new strategies enable more refined, controllable, and multifunctional interfacial structure regulation on fiber surfaces, thereby further expanding the application prospects of EMI shielding fibers in fields such as intelligent protection, optical stealth, and multifield response [198–201]. He et al. constructed a nacre-inspired functional layer on the CF surface using ALD technology, realizing the preparation of colored CFs while endowing them with excellent EMI SE_T and optical camouflage characteristics. This study demonstrated that ALD can deposit ultra-thin and uniform inorganic layers on fiber surfaces with precise thickness controllability and excellent interfacial adhesion, making it an effective pathway for achieving multifunctional fiber surfaces (Fig. 11a) [202]. Other studies have shown that aluminum-doped zinc oxide (AZO) films prepared by ALD technology have excellent conductivity (DEZ:TMA ratio = 15:1, 1.053 mΩ cm), which can enhance the interfacial adhesion of the coating while achieving electromagnetic shielding mainly through conductive loss [203]. Additionally, Chen et al. utilized laser etching to in situ induce the generation of laser-induced graphene (LIG) on the surface of BF-reinforced composites, which not only enhanced the material's EMI shielding performance but also enabled visual detection of impact damage. This research showcased the advantage of laser etching for the rapid, non-contact construction of conductive networks on inorganic fiber surfaces, opening new directions for the intelligence and multifunctionality of EMI shielding composites (Fig. 11b) [204].

Compared to emerging high-precision methods like ALD and laser etching, although dipping is not novel in technical principle, it remains a highly potential functionalization means due to the simple process, low cost, and suitability for large-area continuous processing [205, 206]. As shown in Fig. 11c, Liu et al. prepared free-standing CFFs using an MWCNT dip-coating method, significantly enhancing their EMI shielding efficiency. This method is simple to operate, scalable, and can impart excellent conductivity and EMI shielding performance to the fabric while maintaining its flexibility, demonstrating the application potential of dipping as an efficient coating strategy for functionalizing fibers [207].

Although SE is a crucial performance indicator, the actual EMI shielding materials must also meet various requirements, such as flexibility, cost-effectiveness, and environmental stability. However, these characteristics often have trade-offs with EMI shielding performance (Table 4). It is worth noting that the reported EMI SE values of IHPF-based composites in different studies are often not directly comparable due to variations in testing standards and conditions. The most commonly used testing methods include ASTM D4935-18, IEEE-STD 299, and GB/T 12190, which differ in sample size, holder geometry, and frequency range (typically 8–12 GHz, 12–18 GHz, or broader). Moreover, parameters such as sample thickness, measurement configuration

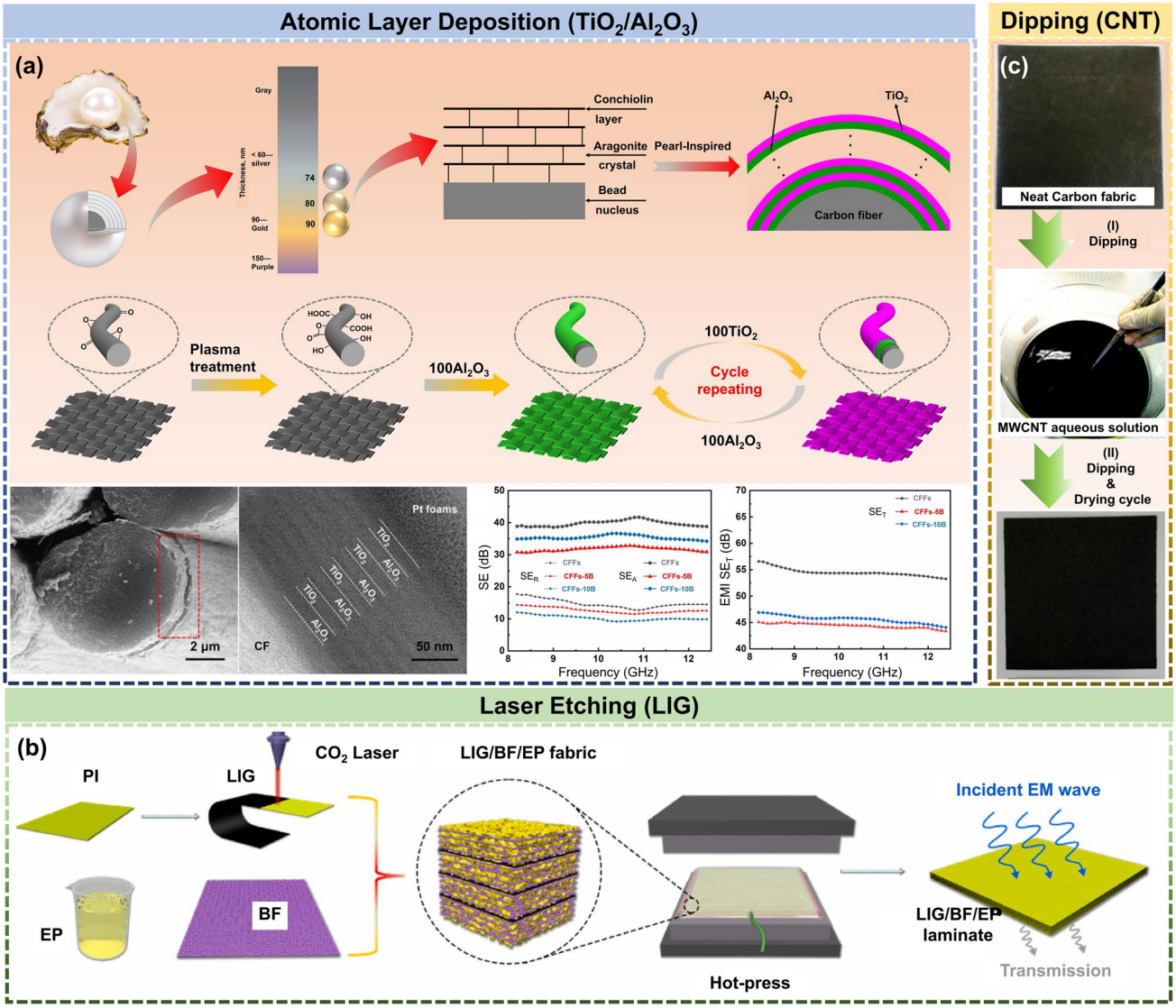

Fig. 11 Other and emerging technologies: ALD, laser etching, and dipping methods are used to fabricate EMI shielding functional layers. **a** Schematic illustration, cross section SEM images, and HRTEM image for colored CF with good EMI shielding property through bio-inspired pearls. Reproduced with permission from [202]. Copyright 2025, John Wiley & Sons; **b** Schematic illustration of the fabrication process of laser-induced graphene inserted BF-reinforced epoxy laminates. Reproduced with permission from [204]. Copyright 2023, Elsevier B.V.; **c** C/C composites were manufactured by dip-coating technique, which is suitable for large-scale preparation. Reproduced with permission from [205]. Copyright 2016, Springer Nature

(coaxial transmission line; waveguide), and surface roughness can significantly influence the measured SE by altering reflection and absorption ratios. Consequently, comparing absolute SE values across different works may lead to misleading conclusions unless these variables are carefully normalized. To improve data consistency and comparability, it is recommended that future reports clearly specify the test standard, frequency range, incident wave direction, and sample thickness, and preferably include normalized parameters such as SSE, SE/t, or SSE/t. Establishing such standardized reporting practices will facilitate fair benchmarking and accelerate the rational design of EMI shielding IHPFs.

In summary, the EMI shielding functionalization of IHPFs and their fabrics primarily relies on various surface coating preparation strategies. Different processes have their own advantages and limitations in terms of coating composition control, interfacial adhesion, process cost, and scalability. From an interface engineering

© The authors https://doi.org/10.1007/s40820-025-02053-z

perspective, the performance and durability of EMI shielding IHPFs are predominantly determined by the chemical and physical attributes of the fiber–coating interface. Chemically, the intrinsic inertness of inorganic fibers often results in insufficient bonding with metallic, carbonaceous, or polymeric coatings, leading to weak interfacial adhesion and potential delamination under mechanical or thermal stress. Physically, mismatches in thermal expansion coefficients, surface morphology, and elastic moduli between the fiber substrate and the functional layer can induce microcracking, stress concentration, and interfacial failure during service. These challenges become even more pronounced in multilayer heterogeneous architectures, where repeated thermal or moisture cycling can accelerate interfacial degradation. Therefore, the future development trend lies in combining multiple strategies, conducting effective interface engineering through surface activation, gradient coating design, and atomic-level conformal deposition (such as ALD) and other approaches, to construct multifunctional electromagnetic shielding fiber materials with high efficiency, lightweight, durability, and multifield response capabilities.

5 Application for EMI Shielding Inorganic High-Performance Fibers/Fabrics

Strategies to address common challenges such as surface inertness in IHPFs are increasingly mature. Various methods for preparing functional surface coatings, including physical deposition, chemical treatments, and emerging surface modification technologies, continue to be refined. This not only provides insights for improving the interfacial bonding between fibers and functional layers but also establishes a robust processing foundation for developing composite fiber materials that integrate excellent mechanical properties with effective EMI shielding performance. Against this backdrop, EMI shielding materials based on IHPFs have gradually transitioned from laboratory exploration to practical applications, demonstrating broad prospects in several critical fields. Specifically, their applications mainly include EMI shielding textiles, wave-absorbing stealth materials, protection for precision equipment, and specialized cables (Fig. 12).

5.1 EMI Shielding for Protection

EMI shielding textiles represent one of the most direct application avenues, widely used in products such as protective clothing, shielding curtains, and flexible shielding layers. Traditional shielding methods mostly use metals, which are not only costly, heavy, and have poor flexibility, but also not corrosion-resistant and require regular maintenance. In contrast, EMI shielding textiles based on IHPF combine structural stability with flexibility and environmental robustness. By depositing metals, conductive polymers, or magnetic materials onto fiber-based fabrics, the EM SE_T can be significantly enhanced while maintaining the fabric's flexibility and breathability. CF has been widely studied and applied due to its excellent mechanical properties, conductivity, and flexibility as fabric. Mei et al. employed electroless silver plating and one-step electrodeposition techniques to develop a flexible superhydrophobic EMI shielding fabric (CEF-NF/PDA/Ag/50–30) based on polydopamine (PDA)-modified CF nonwoven fabric (CEF-NF). This fabric exhibited a SE_T of up to 101.27 dB in the X-band, along with a superhydrophobic surface (contact angle of 156.4°) and good breathability, making it suitable for long-term use in complex environments [208]. Fan et al. combined hydrophobic flame-retardant aramid fabric (FH-Al), porous flame-retardant finished carbonized waste cotton (CR-WCN), and carbon fiber nonwoven (CFN) using a simple sewing process to prepare a multifunctional aluminum-flammability carbonized waste cotton-carbon felt (A-FCWCF) composite fabric, which has excellent development prospects. In addition, when the A-FCWCF composite fabric's thickness is 6 mm, the EMI SE_T reaches 82.63 dB, meeting the requirement of military EMI shielding materials above 75 dB [209]. In addition, BFs also demonstrate broad application prospects in the textile industry due to their mechanical properties, thermal resistance, and corrosion resistance. Xu et al. modified BFFs with functionalized anthraquinone polyurethane (WAPU) coating to produce purple BFFs with excellent wear resistance and EMI shielding function. The modified yarn did not break until 25,000 cycles, which increased the cycle life by 1462.5% compared to the original BF. The fabric maintained thermal and moisture comfort after treatment. Moreover, the WAPU/Ag coated fabric's EMI SE_T reaches 41.1 dB in the X-band range [210]. Protective garments made from such materials can effectively block EMR, safeguarding personnel in specialized occupations (e.g., medical, aviation, and

Fig. 12 Application for EMI shielding IHPFs: EMI shielding fabrics; absorbing stealth; equipment protection; special cables

military fields) from EM hazards. Furthermore, owing to the excellent heat resistance, flame retardancy, and durability of IHPFs, these materials demonstrate superior overall advantages over traditional metal mesh materials in challenging environments.

In aerospace, defense, and high-end electronic equipment, precision instruments often need to operate stably in environments with strong EM pulses, radiation, and extreme temperatures. EMI shielding layers constructed from IHPFs can effectively isolate external EMI while enhancing service life through excellent thermal stability and corrosion resistance. For instance, Xiao et al. significantly improved the EMI shielding performance of SiC fiber-reinforced SiC (SiC_f/SiC) composites via pyrolysis modification using inorganic salts such as $Fe(NO_3)_3$ and $NH_4Al(SO_4)_2$. The study showed that composites with a plain-weave fabric structure modified with Fe elements exhibited optimal shielding performance in the X-band, with SE_T and SE_A reaching 39.29 and 32.36 dB, respectively. The shielding mechanism primarily involved multiple internal reflections and absorption dissipation of EM waves. In satellites, missiles, and avionics systems, multilayer shielding structures based on such modified SiC_f/SiC fabrics can simultaneously achieve lightweight design, high-temperature stability, and strong EM protection. Compared to traditional metal shielding layers, their flexibility and wearability make them more suitable for covering complex structures and irregularly shaped equipment, demonstrating great potential for protecting precision devices in extreme environments.

EMI shielding cables and shielding sleeves are critical components in EM compatibility design, widely used in military communications, rail transportation, and medical electronic equipment. IHPF-based fabrics, owing to their

© The authors https://doi.org/10.1007/s40820-025-02053-z

excellent mechanical properties and abrasion resistance, are ideal skeleton materials for flexible shielding sleeves. When combined with metal or conductive coatings, they effectively reduce EM leakage and signal interference. Moreover, these materials maintain stable performance under extreme conditions, providing reliable protection for critical circuits and data transmission. Gao et al. prepared GO fibers via wet spinning and obtained a series of structurally optimized graphene fibers through chemical reduction and high-temperature annealing, significantly enhancing the electrical conductivity of the fibers. Due to the high EMI shielding performance and flexibility of monolayered textiles woven from graphene fibers, they can be wrapped around cable bundles and protected by heat-shrink tubing, showing potential for applications in daily life and aerospace signal transmission. Furthermore, the standardization and optimization of weaving technology will promote the functional advantages of graphene fiber textiles in EMI shielding, accelerating iterative development in areas such as personal protection and information security.:

5.2 EM Wave-Absorbing Stealth

EM wave absorption and stealth technology are core requirements in aerospace and defense applications. Generally, electromagnetic shielding materials mainly suppress EMI through the reflection of conductive layers and multiple scattering, blocking the transmission of electromagnetic waves. On the other hand, electromagnetic wave absorption materials focus on converting incident electromagnetic energy into heat or other forms through dielectric and magnetic loss mechanisms, thereby minimizing secondary reflections and achieving radar stealth performance [211–218]. When combined with magnetic particles, carbon-based nanomaterials, or dielectric materials, IHPFs can form lightweight, broadband wave-absorbing structures used for EM stealth in fighter aircraft, drones, and naval vessels. Luo et al. coated magnetic Fe-Co alloy on CF's surface (FeCo@CFs) through electroplating. By adjusting the electroplating temperature at 25, 35, and 50 °C, they obtained thin plates, irregular particles, and pyramids as Fe-Co coating morphologies, and FeCo@CFs with different coating morphologies exhibited different magnetic and complex dielectric constants. Among them, FeCo@CFs with a thin plate morphology showed the best absorption performance of 37.7 dB at 2–18 GHz [219]. Liu et al. successfully prepared CF/epoxy composites with tunable electrical conductivity by controlling the temperature and duration during the low-temperature carbonization stage of polyacrylonitrile (PAN) pre-oxidized fibers. This approach enabled a shift from traditional EM shielding to highly efficient microwave absorption. By precisely regulating the microstructure and graphitization degree of the CFs, the impedance matching performance was significantly improved, resulting in excellent wave-absorbing properties across multiple frequency bands [220]. Despite their promise as green and multifunctional EMI protection solutions, absorption-based systems also face several intrinsic limitations. Their absorption bandwidths are often restricted by impedance matching constraints and frequency-selective losses, making broadband absorption challenging under variable electromagnetic conditions. Moreover, thermal management becomes critical under high-power irradiation, as excessive heat accumulation may lead to thermal runaway, degradation of matrix resins, or magnetic loss saturation. In comparison, reflection-dominated systems, though less "stealthy," generally offer higher stability and better heat dissipation in extreme aerospace environments due to their metallic continuity and higher thermal conductivity. Therefore, future research should focus on synergistically integrating absorption and reflection mechanisms to achieve both broadband EM attenuation and thermal robustness, fulfilling the stringent operational requirements of next-generation aerospace and defense platforms.

5.3 Service Reliability and Environmental Stability

As everyone knows, the long-term reliability and environmental stability of EMI shielding IHPFs are critically governed by interfacial integrity and environmental degradation mechanisms. Common failure modes include delamination, oxidation, and fatigue cracking of coating layers under mechanical or thermal stress. "Wet" chemical coatings are prone to hydrolytic degradation, while metallic layers may suffer oxidation-induced conductivity loss. Strategies such as ALD barrier coatings, gradient architectures, and surface coupling agents have been shown to mitigate these effects. Systematic durability testing—such as cyclic bending, thermal shock, and salt spray exposure—is essential for establishing the correlation between microstructural stability and macroscopic shielding performance. Overall, understanding and addressing

degradation mechanisms are essential foundations for the practical deployment of EMI shielding IHPFs in advanced engineering systems.

In summary, EMI shielding materials based on IHPFs show broad application prospects in flexible textiles, wave-absorbing stealth, precision equipment protection, and specialized cables. However, in practical applications, there are many challenges regarding the long-term reliability and environmental stability of EMI shielding IHPF-based composites. The interfaces among fibers, functional coatings, and matrix resins represent the most critical yet vulnerable regions, where cyclic thermal loads, mechanical vibrations, and humid environments can induce microcracking, delamination, or oxidation. Accordingly, precise chemical and physical interface engineering is indispensable to achieve large-scale practical engineering applications and maintain functionality under complex operating conditions. Techniques such as ALD for conformal nanocoating, gradient interfacial architectures for stress relaxation, and coupling-agent-assisted bonding for enhanced chemical compatibility have demonstrated significant improvements in adhesion strength and mitigation of interfacial degradation. By integrating these interfacial optimization approaches into both fabrication and application processes, IHPF-based EMI shielding materials can attain superior durability, multifunctionality, and environmental resilience—bridging the gap between laboratory demonstrations and real-world implementation in aerospace and defense systems. In the future, with continued advancements in multifunctional coating technology, IHPFs are expected to play an even more critical role in integrated systems for EM shielding, protection, and intelligent monitoring.

6 Summary and Outlook

Owing to their lightweight nature, high specific strength, high modulus, and excellent environmental stability, IHPFs have become indispensable key materials in extreme environments such as aerospace and defense/military applications. They provide cutting-edge solutions for related equipment in terms of lightweight design, high durability, and multifunctionality. This review briefly introduces the mechanisms of EMI shielding, highlights common issues such as the surface inertness of IHPFs, and elaborates on both “dry” and “wet” surface modification strategies. These modification strategies enable the construction of robust functional layers on the fiber surfaces, integrating high strength, high modulus, and multifunctionality, while ensuring the interfacial reliability and stability of the composites. Subsequently, we reviewed the principles and processes of various preparation strategies for constructing EMI shielding functional layers on fiber surfaces, discussed in depth how different methods tailor the EM parameters and microstructure of the materials, and summarized the application progress of EMI shielding functionalized IHPFs in areas such as EMI shielding textiles, wave-absorbing stealth, precision equipment protection, and specialized cables.

The development of IHPFs has achieved remarkable accomplishments over the past few decades. Their exceptional mechanical properties, favorable cost-effectiveness, and potential for multifunctional integration have gradually established them as crucial components of a new generation of advanced composite materials. With the growing severity of EMI and EMR issues, the strategic value of EMI shielding functionalization for IHPFs in extreme environments has become increasingly prominent. However, several key challenges require breakthroughs to facilitate their large-scale and long-term application in high-precision and advanced fields: (1) Further optimization of material design and structure is needed to ensure the long-term stability of the interfaces between the functional layer and the fiber, and between the fiber and the resin matrix. (2) Strategies for functional design and processing must be refined to maintain excellent mechanical properties while balancing EMI shielding and absorption performance. (3) Functional layers need to evolve beyond single shielding functions toward the integrated synergy of EMI shielding, absorption, and other multifunctional capabilities. (4) Cost control and the realization of scalable manufacturing are essential alongside the functionalization process. (5) A shift from shielding modes relying solely on EM wave reflection toward absorption-dominated green shielding modes is necessary to achieve environmental friendliness and sustainable development (Fig. 13).

Addressing these challenges requires a multidimensional strategy that simultaneously considers interfacial design, structural optimization, multifunctional coupling, and green manufacturing. Firstly, while surface modification strategies can construct functional layers on fibers, these interfaces may still face issues like delamination, aging, and performance degradation in complex service environments. Future

© The authors https://doi.org/10.1007/s40820-025-02053-z

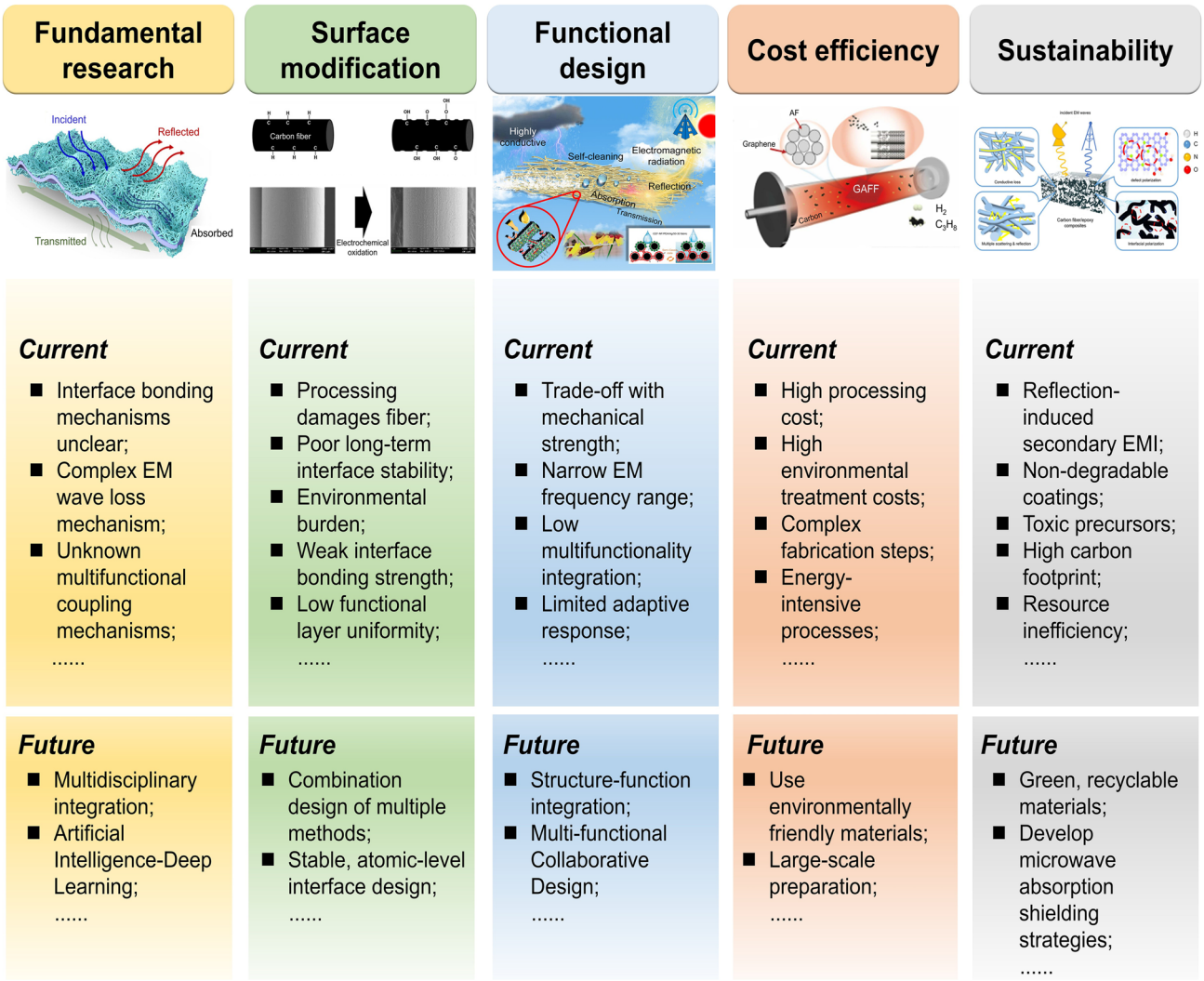

Fig. 13 Summary of current research progress and future challenges and perspectives for EMI shielding IHPF-based materials

research should focus on optimizing the multiscale interfacial structure design between the fiber-functional layer and the fiber-resin matrix. Rational design of hierarchical and hybrid IHPFs that integrate conductive, magnetic, and dielectric components at multiple scales will be essential. Tailoring fiber composition, coating uniformity, and interfacial compatibility can help balance SE, mechanical robustness, and flexibility. Data-driven modeling and machine-learning-assisted design may further accelerate the discovery of optimal structures. For instance, combining techniques like plasma activation and atomic layer deposition to introduce chemical bonds or gradient transition layers could achieve dual assurance of chemical and mechanical stability at the interface.

Secondly, regarding the balance between mechanical properties and EMI functionality, overly thick or dense functional layers often compromise the specific strength and modulus of the fibers, while focusing solely on mechanical performance makes it difficult to achieve ideal SE. Therefore, there is an urgent need to develop functionalization strategies that offer structural controllability, lightweight, and high efficiency. Constructing ultra-thin nanocoatings, layered conductive networks, or hierarchical porous structures holds promise for granting excellent EM regulation capabilities while preserving mechanical properties, thereby

achieving the synergistic optimization of "lightweight-high strength-efficient shielding".

In addition, traditional EMI shielding primarily relies on single mechanisms like reflection or absorption. In practical applications, fiber functional layers must simultaneously address multiple demands such as mechanical reinforcement, thermal protection, corrosion resistance, and optical response. The future trend involves utilizing multiscale interface regulation and heterogeneous material synergy design to integrate EMI shielding and wave absorption performance with thermal management, fire retardancy, and sensing functionalities. However, achieving such integration inevitably introduces trade-offs between conductivity, flexibility, and strength, requiring optimized microstructures and interfacial architectures to maintain balanced performance. For instance, composites of carbon-based conductive materials (CF, CNT fiber, etc.) with metal oxides or conductive polymers can achieve coupled multimechanisms and synergistic enhancement of multiple properties.

Furthermore, concerning scalable manufacturing and cost control, while laboratory-scale techniques such as electroless plating, ALD, and CVD provide precise control at the laboratory level, their cost, industrial scalability, and energy efficiency remain critical challenges. Efforts should promote the development of green, efficient, and low-energy consumption preparation processes. Employing roll-to-roll deposition techniques, atmospheric pressure ALD, or combining spraying/dipping with microwave curing processes can enhance production efficiency and reduce costs while maintaining performance. Simultaneously, standardized testing and evaluation systems suitable for industrial production should be explored to ensure the consistency and controllability of functional fiber performance in large-scale manufacturing, thereby accelerating their practical application in aerospace, defense, and civilian sectors.

Finally, environmental friendliness and sustainability considerations must guide future material and process design. Traditional wet-chemical routes often generate chemical waste, whereas vapor-phase methods (e.g., ALD or roll-to-roll CVD) are energy-intensive. Future research should focus on developing green raw materials and biodegradable/recyclable processes. Reducing chemical emissions, utilizing recyclable or bio-based components, and adopting solvent-free coating methods will minimize environmental impact. Lightweight and corrosion-resistant IHPFs also contribute to energy savings and longer service lifetimes, aligning with green manufacturing principles. Developing low-energy, continuous, and environmentally benign processes will be vital for industrial translation. Moreover, a more critical issue is that traditional EMI shielding often relies on high-reflectivity materials, which leads to the problem of secondary scattering of EM pollution. Future research emphasis should shift toward absorption-based EMI shielding strategies, such as introducing magnetic loss, dielectric loss, and multiple scattering mechanisms to enhance the effective dissipation of EM energy. Concurrently, developing green shielding fibers based on renewable resources, low-carbon processes, and recyclable materials will contribute to advancing EM protective materials toward environmental friendliness and sustainable development.

In summary, these ongoing developments highlight that IHPFs possess immense potential for EMI shielding functionalization and beyond. However, their large-scale application in extreme environments is still constrained by multiple challenges, including interfacial stability, the coupling of mechanical and EM properties, multifunctional integration, scalable manufacturing, and green sustainability. Future development trends should focus on multiscale interface regulation and structural design, utilizing advanced processes to construct efficient functional layers while balancing lightweight and mechanical performance. For multifunctional synergy, exploring the integration of EMI shielding with thermal management, fire retardancy, sensing, and other properties is essential to meet multiple demands in complex environments and achieve functional customization. At the process level, there is a need to develop green, low-cost, and continuous functionalization technologies to facilitate the transition from laboratory research to industrial application. It is foreseeable that with continuous breakthroughs in new material systems and multidimensional structural design, the EMI shielding functionalization of IHPFs will play an increasingly vital role in aerospace, national defense security, and the next generation of intelligent electronic protection fields.

Acknowledgements National Natural Science Foundation of China (52373085, 52573090, 52533017 and U21A2095), Department of Science and Technology of Hubei Province (No. 2025CSA001 and 2024CSA076), Outstanding Young and Middle-aged Scientific and Technology Innovation Team of Higher Education Institutions of Hubei Province (No. T2024010), Innovative Team Program of Natural Science Foundation of Hubei Province (No. 2023AFA027), Major Fundamental Research of Natural Science Foundation of Shandong Province (ZR2025ZD33) and

© The authors https://doi.org/10.1007/s40820-025-02053-z

Technical Support Project of Administration for Market Regulation of Hubei Province (Hbscjg-JS2025001).

Author Contributions Sijie Qiao contributed to investigation and original draft writing. Zhicheng Shi performed investigation and editing. Aixin Tong, Zhiyu Huang, and Annan He performed review and editing. Binhao Wang, Jun He, Jiaxin Wang, Ming Chen, Zixi Huang, Linhui Hao, and Bing Wu edited the manuscript. Yan Jun, Ya-Lan Tan, Pibo Ma, Weilin Xu, and Fengxiang Chen contributed to conceptualization, supervision, and funding acquisition.

Declarations

Conflict of interest The authors declare that they have no known competing financial interests or personal relationships that could have appeared to influence the work reported in this paper.

Open Access This article is licensed under a Creative Commons Attribution 4.0 International License, which permits use, sharing, adaptation, distribution and reproduction in any medium or format, as long as you give appropriate credit to the original author(s) and the source, provide a link to the Creative Commons licence, and indicate if changes were made. The images or other third party material in this article are included in the article's Creative Commons licence, unless indicated otherwise in a credit line to the material. If material is not included in the article's Creative Commons licence and your intended use is not permitted by statutory regulation or exceeds the permitted use, you will need to obtain permission directly from the copyright holder. To view a copy of this licence, visit http://creativecommons.org/licenses/by/4.0/.

References

1. D. Tao, X. Wen, C. Yang, K. Yan, Z. Li et al., Controlled twill surface structure endowing nanofiber composite membrane excellent electromagnetic interference shielding. Nano-Micro Lett. **16**(1), 236 (2024). https://doi.org/10.1007/s40820-024-01444-y
2. J. Liu, M.-Y. Yu, Z.-Z. Yu, V. Nicolosi, Design and advanced manufacturing of electromagnetic interference shielding materials. Mater. Today **66**, 245–272 (2023). https://doi.org/10.1016/j.mattod.2023.03.022
3. A. Liu, H. Qiu, X. Lu, H. Guo, J. Hu et al., Asymmetric structural MXene/PBO aerogels for high-performance electromagnetic interference shielding with ultra-low reflection. Adv. Mater. **37**(5), e2414085 (2025). https://doi.org/10.1002/adma.202414085
4. W. Zhao, M. Li, Z. Zhang, H.-X. Peng, EMI shielding effectiveness of silver nanoparticle-decorated multi-walled carbon nanotube sheets. Int. J. Smart Nano Mater. **1**(4), 249–260 (2010). https://doi.org/10.1080/19475411.2010.511477
5. C. Liang, Z. Gu, Y. Zhang, Z. Ma, H. Qiu et al., Structural design strategies of polymer matrix composites for electromagnetic interference shielding: a review. Nano-Micro Lett. **13**(1), 181 (2021). https://doi.org/10.1007/s40820-021-00707-2
6. Z. Shi, Z. Liang, Z. Huang, A. He, S. Qiao et al., Revolutionizing fiber materials for space: multi-scale interface engineering unlocks new aerospace frontiers. Mater. Today **88**, 643–704 (2025). https://doi.org/10.1016/j.mattod.2025.06.010
7. W. Lu, M. Zu, J.-H. Byun, B.-S. Kim, T.-W. Chou, State of the art of carbon nanotube fibers: opportunities and challenges. Adv. Mater. **24**(14), 1805–1833 (2012). https://doi.org/10.1002/adma.201104672
8. G. Xin, T. Yao, H. Sun, S.M. Scott, D. Shao et al., Highly thermally conductive and mechanically strong graphene fibers. Science **349**(6252), 1083–1087 (2015). https://doi.org/10.1126/science.aaa6502
9. L. Chen, Y. He, S. Chai, H. Qiang, F. Chen et al., Toward high performance graphene fibers. Nanoscale **5**(13), 5809 (2013). https://doi.org/10.1039/c3nr01083j
10. P.-Y. Hung, K.T. Lau, Q. Guo, B. Jia, B. Fox, Tailoring specific properties of polymer-based composites by using graphene and its associated compounds. Int. J. Smart Nano Mater. **11**(2), 173–189 (2020). https://doi.org/10.1080/19475411.2020.1786477
11. V. Dhand, G. Mittal, K.Y. Rhee, S.-J. Park, D. Hui, A short review on basalt fiber reinforced polymer composites. Compos. Part B Eng. **73**, 166–180 (2015). https://doi.org/10.1016/j.compositesb.2014.12.011
12. B. Mainzer, C. Lin, M. Frieß, R. Riedel, J. Riesch et al., Novel ceramic matrix composites with tungsten and molybdenum fiber reinforcement. J. Eur. Ceram. Soc. **41**(5), 3030–3036 (2021). https://doi.org/10.1016/j.jeurceramsoc.2019.10.049
13. Y. Mao, J. Coenen, S. Sistla, C. Liu, A. Terra et al., Design of tungsten fiber-reinforced tungsten composites with porous matrix. Mater. Sci. Eng. A **817**, 141361 (2021). https://doi.org/10.1016/j.msea.2021.141361
14. V.E. Ogbonna, A.P.I. Popoola, O.M. Popoola, S.O. Adeosun, A review on corrosion, mechanical, and electrical properties of glass fiber-reinforced epoxy composites for high-voltage insulator core rod applications: challenges and recommendations. Polym. Bull. **79**(9), 6857–6884 (2022). https://doi.org/10.1007/s00289-021-03846-z
15. H. Liu, Y. Sun, Y. Yu, M. Zhang, L. Li et al., Effect of nano-SiO_2 modification on mechanical and insulation properties of basalt fiber reinforced composites. Polymers **14**(16), 3353 (2022). https://doi.org/10.3390/polym14163353
16. L. Xie, Y. Han, Y. Huang, Study on the effect of heat treatment on the structure, mechanical and electrical properties of alumina fiber insulation. J. Phys. D Appl. Phys. **57**(42), 425401 (2024). https://doi.org/10.1088/1361-6463/ad6456
17. M. Sharma, S. Gao, E. Mäder, H. Sharma, L.Y. Wei et al., Carbon fiber surfaces and composite interphases. Compos. Sci. Technol. **102**, 35–50 (2014). https://doi.org/10.1016/j.compscitech.2014.07.005
18. C.-P. Ma, Y. Zhang, H. Zhang, A.-J. Gao, Y. Wang, Effects of acid–base properties of ammonium salt electrolyte on electrochemical surface activation of carbon fibers. Fibers

Polym. **24**(10), 3501–3511 (2023). https://doi.org/10.1007/s12221-023-00322-5

19. T. Ma, R. Shao, A. Siddique, W. Wang, T. Li et al., Repairing surface defects of carbon fibers: electrostatic spraying nanocarbons on stabilized PAN-fibers and subsequent thermal annealing. Surf. Interfaces **52**, 104783 (2024). https://doi.org/10.1016/j.surfin.2024.104783
20. A. Stolle, B. Ondruschka, I. Morgenthal, O. Andersen, W. Bonrath, Metallic short fibers for liquid-phase oxidation reactions. J. Mol. Catal. A Chem. **335**(1–2), 228–235 (2011). https://doi.org/10.1016/j.molcata.2010.11.038
21. Y. Wang, Z. Wang, X. Wang, H. Liu, Y. Ma et al., The effect of liquid-phase preoxidation on the use of carbon fibers in Al_2O_3-C refractories. Int. J. Appl. Ceram. Technol. **22**(5), e15160 (2025). https://doi.org/10.1111/ijac.15160
22. X. Qian, X. Wang, Q. OuYang, Y. Chen, Q. Yan, Surface structural evolvement in electrochemical oxidation and sizing and its effect on carbon fiber/epoxy composites properties. J. Reinf. Plast. Compos. **31**(15), 999–1008 (2012). https://doi.org/10.1177/0731684412449895
23. X. Qian, J. Zhi, L. Chen, J. Huang, Y. Zhang, Effect of low current density electrochemical oxidation on the properties of carbon fiber-reinforced epoxy resin composites. Surf. Interface Anal. **45**(5), 937–942 (2013). https://doi.org/10.1002/sia.5185
24. Y. Luo, Y. Zhang, T. Xing, A. He, S. Zhao et al., Full-color tunable and highly fire-retardant colored carbon fibers. Adv. Fiber Mater. **5**(5), 1618–1631 (2023). https://doi.org/10.1007/s42765-023-00294-4
25. F. Chen, Y. Huang, R. Li, S. Zhang, Q. Jiang et al., Superdurable and fire-retardant structural coloration of carbon nanotubes. Sci. Adv. **8**(26), eabn5882 (2022). https://doi.org/10.1126/sciadv.abn5882
26. Z. Dai, F. Shi, B. Zhang, M. Li, Z. Zhang, Effect of sizing on carbon fiber surface properties and fibers/epoxy interfacial adhesion. Appl. Surf. Sci. **257**(15), 6980–6985 (2011). https://doi.org/10.1016/j.apsusc.2011.03.047
27. C. Ralph, P. Lemoine, A. Boyd, E. Archer, A. McIlhagger, The effect of fibre sizing on the modification of basalt fibre surface in preparation for bonding to polypropylene. Appl. Surf. Sci. **475**, 435–445 (2019). https://doi.org/10.1016/j.apsusc.2019.01.001
28. Y.-S. Wei, X.-Z. Huang, Z.-J. Du, Y. Cheng, Synthesis of BN coatings on carbon fiber by dip coating. Surf. Interface Anal. **49**(3), 177–181 (2017). https://doi.org/10.1002/sia.6105
29. G. Zhang, W. Yang, J. Ding, M. Liu, C. Di et al., Influence of carbon fibers on interfacial bonding properties of copper-coated carbon fibers. Carbon Lett. **34**(3), 1055–1064 (2024). https://doi.org/10.1007/s42823-023-00671-4
30. A.S. Nitai, T. Chowdhury, M.N. Inam, M.S. Rahman, M.I.H. Mondal et al., Carbon fiber and carbon fiber composites: creating defects for superior material properties. Adv. Compos. Hybrid Mater. **7**(5), 169 (2024). https://doi.org/10.1007/s42114-024-00971-x
31. O. Dagdag, H. Kim, Advances in flame retardant technologies for epoxy resins: chemical grafting onto carbon fiber techniques, reactive agents, and applications in composite materials. Molecules **29**(24), 5996 (2024). https://doi.org/10.3390/molecules29245996
32. L. Yang, H. Xia, Z. Xu, L. Zou, Q. Ni, Influence of surface modification of carbon fiber based on magnetron sputtering technology on mechanical properties of carbon fiber composites. Mater. Res. Express **7**(10), 105602 (2020). https://doi.org/10.1088/2053-1591/abbc90
33. L. Yang, Y. Chen, Z. Xu, H. Xia, T. Natuski et al., Effect of surface modification of carbon fiber based on magnetron sputtering technology on tensile properties. Carbon **204**, 377–386 (2023). https://doi.org/10.1016/j.carbon.2022.12.045
34. W. Wang, J. Li, J. Shi, Y. Jiao, X. Wang et al., Structure and physical properties of conductive bamboo fiber bundle fabricated by magnetron sputtering. Materials **16**(8), 3154 (2023). https://doi.org/10.3390/ma16083154
35. S. Lu, X. Yang, L. Zhang, J. Ma, S. Wang et al., Real-time monitoring of resin infiltration process in vacuum assisted molding(VARI) of composites with carbon nanotube buckypaper sensor. Mater. Res. Express **6**(11), 115628 (2019). https://doi.org/10.1088/2053-1591/ab507b
36. Z. Wang, L. Zhang, X. Liu, X. Dong, L. Yang et al., Basalt flake/epoxy resin nacre-inspired bulk composite fabricated by vacuum-assisted resin transfer molding technique. Mater. Lett. **384**, 138122 (2025). https://doi.org/10.1016/j.matlet.2025.138122
37. D. Chen, C. Liu, Z. Kang, Thin copper hybrid structures by spray-assisted layer by layer chemical deposition on fabric surfaces for electromagnetic interference shielding. Colloid Interface Sci. Commun. **40**, 100365 (2021). https://doi.org/10.1016/j.colcom.2021.100365
38. S. Hwang, C.C. Walker, D. Johnson, Y. Han, D.J. Gardner, Spray drying enzyme-treated cellulose nanofibrils. Polymers **15**(20), 4086 (2023). https://doi.org/10.3390/polym15204086
39. J. Zhang, S. Liu, J. Liu, Y. Lu, Y. Liu et al., Electroless nickel plating and spontaneous infiltration behavior of woven carbon fibers. Mater. Des. **186**, 108301 (2020). https://doi.org/10.1016/j.matdes.2019.108301
40. J.N. Balaraju, P. Radhakrishnan, V. Ezhilselvi, A.A. Kumar, Z. Chen et al., Studies on electroless nickel polyalloy coatings over carbon fibers/CFRP composites. Surf. Coat. Technol. **302**, 389–397 (2016). https://doi.org/10.1016/j.surfcoat.2016.06.040
41. R.H. Guo, S.X. Jiang, C.W.M. Yuen, M.C.F. Ng, J.W. Lan et al., Influence of deposition parameters and kinetics of electroless Ni-P plating on polyester fiber. Fibers Polym. **13**(8), 1037–1043 (2012). https://doi.org/10.1007/s12221-012-1037-4
42. J. Li, S. Bi, B. Mei, F. Shi, W. Cheng et al., Effects of three-dimensional reduced graphene oxide coupled with nickel nanoparticles on the microwave absorption of carbon fiber-based

© The authors

composites. J. Alloys Compd. **717**, 205–213 (2017). https://doi.org/10.1016/j.jallcom.2017.03.098

43. W. Wang, Z. Zhai, J. Liu, Y. Wang, Z. Yang, Influence of carbon fiber nickel electroplating on the electromagnetic interference shielding and mechanical properties of carbon fiber reinforced polyamide 6 composites. Polym. Compos. **44**(12), 8838–8848 (2023). https://doi.org/10.1002/pc.27741
44. J. Zeng, X. Ji, Y. Ma, Z. Zhang, S. Wang et al., 3D graphene fibers grown by thermal chemical vapor deposition. Adv. Mater. **30**(12), e1705380 (2018). https://doi.org/10.1002/adma.201705380
45. X. Luo, S. Wu, Y.-Q. Yang, N. Jin, S. Liu et al., Deposition of titanium coating on SiC fiber by chemical vapor deposition with Ti-I_2 system. Appl. Surf. Sci. **406**, 62–68 (2017). https://doi.org/10.1016/j.apsusc.2017.02.141
46. Z.-X. Chen, C. Chang, X. Yue, H. Li, C.-G. Liang et al., Experimental and theoretical study on the electromagnetic shielding performance of polymer nanocomposites consisting of basalt fiber and CNTs. Compos. Sci. Technol. **247**, 110399 (2024). https://doi.org/10.1016/j.compscitech.2023.110399
47. Z. Wang, Y. Dong, J.-C. Yang, X.-J. Wang, M.-L. Zhang et al., Improved interfacial shear strength in carbon fiber enhanced semi-aromatic polyamide 6T composite via in situ polymerization on fiber surface. Compos. Sci. Technol. **223**, 109401 (2022). https://doi.org/10.1016/j.compscitech.2022.109401
48. H. Li, Z. Sha, Y. Song, J. Fan, J. Wei et al., Developing wearable photothermal and antibacterial fabrics: In-situ polymerization of MoS2-hybridized PET fibers. Compos. Sci. Technol. **270**, 111291 (2025). https://doi.org/10.1016/j.compscitech.2025.111291
49. E. Fedorenko, G.A. Luinstra, In situ polymerization and synthesis of UHMWPE/carbon fiber composites. Polymers **17**(1), 90 (2025). https://doi.org/10.3390/polym17010090
50. K. Mosnáčková, M.M. Chehimi, P. Fedorko, M. Omastová, Polyamide grafted with polypyrrole: formation, properties, and stability. Chem. Pap. **67**(8), 979–994 (2013). https://doi.org/10.2478/s11696-012-0305-5
51. H. Fang, L. Yuan, G. Liang, A. Gu, Aramid fibre-based wearable electrochemical capacitors with high energy density and mechanical properties through chemical synergistic combination of multi-coatings. Electrochim. Acta **284**, 149–158 (2018). https://doi.org/10.1016/j.electacta.2018.07.155
52. S. Qiao, Z. Shi, A. Tong, Y. Luo, Y. Zhang et al., Atomic layer deposition paves the way for next-generation smart and functional textiles. Adv. Colloid Interface Sci. **341**, 103500 (2025). https://doi.org/10.1016/j.cis.2025.103500
53. S. Qiao, Z. Shi, Y. Zhang, G. Zhang, Z. Huang et al., Colorful polyester with high-efficiency flame retardant and anti-dripping properties. Chem. Eng. J. **521**, 166544 (2025). https://doi.org/10.1016/j.cej.2025.166544
54. F. Chen, H. Yang, K. Li, B. Deng, Q. Li et al., Facile and effective coloration of dye-inert carbon fiber fabrics with tunable colors and excellent laundering durability. ACS Nano **11**(10), 10330–10336 (2017). https://doi.org/10.1021/acsnano.7b05139
55. P. Lorenz, M. Ehrhardt, K. Zimmer, Structuring of glass fibre surfaces by laser-induced front side etching. Appl. Surf. Sci. **302**, 52–57 (2014). https://doi.org/10.1016/j.apsusc.2014.01.045
56. C. Vass, B. Kiss, J. Kopniczky, B. Hopp, Etching of fused silica fiber by metallic laser-induced backside wet etching technique. Appl. Surf. Sci. **278**, 241–244 (2013). https://doi.org/10.1016/j.apsusc.2012.11.163
57. Y. Zhang, J. Gu, A perspective for developing polymer-based electromagnetic interference shielding composites. Nano-Micro Lett. **14**(1), 89 (2022). https://doi.org/10.1007/s40820-022-00843-3
58. X. Hou, X.-R. Feng, K. Jiang, Y.-C. Zheng, J.-T. Liu et al., Recent progress in smart electromagnetic interference shielding materials. J. Mater. Sci. Technol. **186**, 256–271 (2024). https://doi.org/10.1016/j.jmst.2024.01.008
59. J.-M. Thomassin, C. Jérôme, T. Pardoen, C. Bailly, I. Huynen et al., Polymer/carbon based composites as electromagnetic interference (EMI) shielding materials. Mater. Sci. Eng. R. Rep. **74**(7), 211–232 (2013). https://doi.org/10.1016/j.mser.2013.06.001
60. M. Han, C.E. Shuck, R. Rakhmanov, D. Parchment, B. Anasori et al., Beyond $Ti_3C_2T_x$: MXenes for electromagnetic interference shielding. ACS Nano **14**(4), 5008–5016 (2020). https://doi.org/10.1021/acsnano.0c01312
61. Y. Zhuo, Y. Yao, Y. Zhuge, Enhancing electromagnetic shielding performance of cement-based materials using industrial waste copper swarf. Constr. Build. Mater. **426**, 136162 (2024). https://doi.org/10.1016/j.conbuildmat.2024.136162
62. D. Ji, Y. Wang, C. He, K. Cui, P. Han et al., High-efficiency electromagnetic shielding based on multipolar effect in RGO/MXene aerogels decorated with ordered Fe_3O_4 cluster. Carbon **226**, 119189 (2024). https://doi.org/10.1016/j.carbon.2024.119189
63. S.A. Schelkunoff, A mathematical theory of linear arrays. Bell Syst. Tech. J. **22**(1), 80–107 (1943). https://doi.org/10.1002/j.1538-7305.1943.tb01306.x
64. J. Xue, X. Yin, F. Ye, L. Zhang, L. Cheng, Theoretical prediction and experimental verification on EMI shielding effectiveness of dielectric composites using complex permittivity. Ceram. Int. **43**(18), 16736–16743 (2017). https://doi.org/10.1016/j.ceramint.2017.09.067
65. A. Nazir, H. Yu, L. Wang, M. Haroon, R.S. Ullah et al., Recent progress in the modification of carbon materials and their application in composites for electromagnetic interference shielding. J. Mater. Sci. **53**(12), 8699–8719 (2018). https://doi.org/10.1007/s10853-018-2122-x
66. R. Kumar, S. Sahoo, E. Joanni, J.-J. Shim, Cutting edge composite materials based on MXenes: synthesis and electromagnetic interference shielding applications. Compos. Part B Eng. **264**, 110874 (2023). https://doi.org/10.1016/j.compositesb.2023.110874

67. D. Jiang, V. Murugadoss, Y. Wang, J. Lin, T. Ding et al., Electromagnetic interference shielding polymers and nanocomposites - a review. Polym. Rev. **59**(2), 280–337 (2019). https://doi.org/10.1080/15583724.2018.1546737
68. H.-J. Kim, S.-H. Kim, S. Park, Effects of the carbon fiber-carbon microcoil hybrid formation on the effectiveness of electromagnetic wave shielding on carbon fibers-based fabrics. Materials **11**(12), 2344 (2018). https://doi.org/10.3390/ma11122344
69. H. Gao, Y. Wang, W. Xu, Research progress of fiber-based electromagnetic shielding materials. Fibres. Polym. **26**(9), 3689–3713 (2025). https://doi.org/10.1007/s12221-025-01063-3
70. W. Zhang, L. Wei, Z. Ma, Q. Fan, J. Ma, Advances in waterborne polymer/carbon material composites for electromagnetic interference shielding. Carbon **177**, 412–426 (2021). https://doi.org/10.1016/j.carbon.2021.02.093
71. Z. Xiang, Y. Shi, X. Zhu, L. Cai, W. Lu, Flexible and waterproof 2D/1D/0D construction of MXene-based nanocomposites for electromagnetic wave absorption, EMI shielding, and photothermal conversion. Nano-Micro Lett. **13**(1), 150 (2021). https://doi.org/10.1007/s40820-021-00673-9
72. J. Cheng, C. Li, Y. Xiong, H. Zhang, H. Raza et al., Recent advances in design strategies and multifunctionality of flexible electromagnetic interference shielding materials. Nano-Micro Lett. **14**(1), 80 (2022). https://doi.org/10.1007/s40820-022-00823-7
73. F. Deng, J. Wei, Y. Xu, Z. Lin, X. Lu et al., Regulating the electrical and mechanical properties of TaS_2 films *via* van der Waals and electrostatic interaction for high performance electromagnetic interference shielding. Nano-Micro Lett. **15**(1), 106 (2023). https://doi.org/10.1007/s40820-023-01061-1
74. X.-X. Wang, Q. Zheng, Y.-J. Zheng, M.-S. Cao, Green EMI shielding: dielectric/magnetic "genes" and design philosophy. Carbon **206**, 124–141 (2023). https://doi.org/10.1016/j.carbon.2023.02.012
75. X.-X. Wang, J.-C. Shu, W.-Q. Cao, M. Zhang, J. Yuan et al., Eco-mimetic nanoarchitecture for green EMI shielding. Chem. Eng. J. **369**, 1068–1077 (2019). https://doi.org/10.1016/j.cej.2019.03.164
76. X. Jia, Y. Li, B. Shen, W. Zheng, Evaluation, fabrication and dynamic performance regulation of green EMI-shielding materials with low reflectivity: a review. Compos. B Eng. **233**, 109652 (2022). https://doi.org/10.1016/j.compositesb.2022.109652
77. P.P. Singh, A. De, B.B. Khatua, Bio-inspired smart composite architecture for thermally tunable green EMI shielding. Appl. Surf. Sci. **643**, 158643 (2024). https://doi.org/10.1016/j.apsusc.2023.158643
78. D. Munalli, G. Dimitrakis, D. Chronopoulos, S. Greedy, A. Long, Electromagnetic shielding effectiveness of carbon fibre reinforced composites. Compos. B Eng. **173**, 106906 (2019). https://doi.org/10.1016/j.compositesb.2019.106906
79. K. Zdeněk, K. Pavel, P. David, S. Jiří, On the shielding effectiveness calculation. Computing **95**(1), 111–121 (2013). https://doi.org/10.1007/s00607-013-0312-6
80. J.-H. Lee, Y.-S. Kim, H.-J. Ru, S.-Y. Lee, S.-J. Park, Highly flexible fabrics/epoxy composites with hybrid carbon nanofillers for absorption-dominated electromagnetic interference shielding. Nano-Micro Lett. **14**(1), 188 (2022). https://doi.org/10.1007/s40820-022-00926-1
81. G. Mittal, K.Y. Rhee, Hierarchical structures of CNT@basalt fabric for tribological and electrical applications: impact of growth temperature and time during synthesis. Compos. Part A Appl. Sci. Manuf. **115**, 8–21 (2018). https://doi.org/10.1016/j.compositesa.2018.09.006
82. B. Cheng, J. Wang, F. Zhang, S. Qi, Preparation of silver/carbon fiber/polyaniline microwave absorption composite and its application in epoxy resin. Polym. Bull. **75**(1), 381–393 (2018). https://doi.org/10.1007/s00289-017-2035-x
83. J. Zhang, P. Liu, R. Chen, Y. Zhang, K. Jiang, CNT fibers based laminated composites resistant to extreme environments: synergistic design of electromagnetic shielding performance and high-temperature resistance. Mater Charact **227**, 115310 (2025). https://doi.org/10.1016/j.matchar.2025.115310
84. C. Wan, Y. Jiao, X. Li, W. Tian, J. Li et al., A multi-dimensional and level-by-level assembly strategy for constructing flexible and sandwich-type nanoheterostructures for high-performance electromagnetic interference shielding. Nanoscale **12**(5), 3308–3316 (2020). https://doi.org/10.1039/C9NR09087H
85. Q. Xiao, Z. Chen, J. Liao, Y. Li, L. Xue et al., Electromagnetic interference shielding performance and mechanism of Fe/Al modified SiC f/SiC composites. J. Alloys Compd. **887**, 161359 (2021). https://doi.org/10.1016/j.jallcom.2021.161359
86. H. Liu, J. Dang, C. Lei, Z. Zhu, X. Li et al., Modulating interface of Ni-embedded hollow porous $Ti_3C_2T_x$ MXene film toward efficient EMI shielding. Small (2025). https://doi.org/10.1002/smll.202410937
87. Q. Ding, J. Yang, H. Yang, S. Gu, Z. Cheng et al., Superior EMI shielding and thermal management of flexible, fire-resistant SiBCNZr nanofiber fabrics enhanced by defect engineering and graphitization. Adv. Funct. Mater. **35**(9), 2416039 (2025). https://doi.org/10.1002/adfm.202416039
88. R. Verma, P. Thakur, A. Chauhan, R. Jasrotia, A. Thakur, A review on MXene and its' composites for electromagnetic interference (EMI) shielding applications. Carbon **208**, 170–190 (2023). https://doi.org/10.1016/j.carbon.2023.03.050
89. G. Wang, J. Chen, W. Zheng, B. Shen, High-efficiency flexible liquid metal/elastomer composite film with designability for strain-invariant electromagnetic shielding and Joule-heating applications. Chem. Eng. J. **488**, 151052 (2024). https://doi.org/10.1016/j.cej.2024.151052
90. X. Yang, L. Xuan, W. Men, X. Wu, D. Lan et al., Carbonyl iron/glass fiber cloth composites: achieving multi-spectrum stealth in a wide temperature range. Chem. Eng. J. **491**, 151862 (2024). https://doi.org/10.1016/j.cej.2024.151862
91. W.C. Wang, B. Zhou, S.H. Xu, Z.M. Yang, Q.Y. Zhang, Recent advances in soft optical glass fiber and fiber lasers.

© The authors

Prog. Mater. Sci. **101**, 90–171 (2019). https://doi.org/10.1016/j.pmatsci.2018.11.003

92. J. Li, Y. Wang, W. Zhao, P. Xu, T. Wang et al., High-performance quartz fiber/polysilazane and epoxy-modified cyanate ester microwave-transparent composites. Adv. Compos. Hybrid Mater. **5**(3), 1830–1840 (2022). https://doi.org/10.1007/s42114-022-00456-9
93. H. Jamshaid, R. Mishra, A green material from rock: basalt fiber–a review. J. Text. Inst. **107**(7), 923–937 (2016). https://doi.org/10.1080/00405000.2015.1071940
94. P. Jagadeesh, S.M. Rangappa, S. Siengchin, Basalt fibers: an environmentally acceptable and sustainable green material for polymer composites. Constr. Build. Mater. **436**, 136834 (2024). https://doi.org/10.1016/j.conbuildmat.2024.136834
95. H. Jia, Y. Qiao, Y. Zhang, C. Liu, X. Jian, Excellent and effective interfacial transition layer with an organic/inorganic hybrid carbon nanotube network structure for basalt fiber reinforced high-performance thermoplastic composites. Chem. Eng. J. **465**, 142995 (2023). https://doi.org/10.1016/j.cej.2023.142995
96. Y. Zhang, Y. Luo, Y. Huang, M. Wang, A. He et al., Desired color diversity of carbon fiber with excellent environmental super-durability and remarkable flame retardancy. ACS Appl. Mater. Interfaces **17**(5), 8340–8348 (2025). https://doi.org/10.1021/acsami.4c19626
97. Y. Luo, Z. Shi, S. Qiao, A. Tong, X. Liao et al., Advances in nanomaterials as exceptional fillers to reinforce carbon fiber-reinforced polymers composites and their emerging applications. Polym. Compos. **46**(1), 54–80 (2025). https://doi.org/10.1002/pc.29027
98. Y. Zhang, Y. Luo, M. Wang, T. Xing, A. He et al., Advances in colored carbon-based fiber materials and their emerging applications. SusMat **4**(6), e243 (2024). https://doi.org/10.1002/sus2.243
99. K. Koziol, J. Vilatela, A. Moisala, M. Motta, P. Cunniff et al., High-performance carbon nanotube fiber. Science **318**(5858), 1892–1895 (2007). https://doi.org/10.1126/science.1147635
100. B. Fang, D. Chang, Z. Xu, C. Gao, A review on graphene fibers: expectations, advances, and prospects. Adv. Mater. **32**(5), e1902664 (2020). https://doi.org/10.1002/adma.201902664
101. L. Li, X. Liu, G. Wang, Y. Liu, W. Kang et al., Research progress of ultrafine alumina fiber prepared by sol-gel method: a review. Chem. Eng. J. **421**, 127744 (2021). https://doi.org/10.1016/j.cej.2020.127744
102. L. Oppenheimer, M. Ramkumar, I. Machado, C. Scott, S. Winroth et al., Development of an atomic-oxygen-erosion-resistant, alumina-fiber-reinforced, fluorinated polybenzoxazine composite for low-earth orbital applications. Polymers **15**, 112 (2022). https://doi.org/10.3390/polym15010112
103. Y. Lei, Y. Wang, Y. Song, Y. Li, C. Deng et al., Nearly stoichiometric BN fiber with low dielectric constant derived from poly [(alkylamino)borazine. Mater. Lett. **65**(2), 157–159 (2011). https://doi.org/10.1016/j.matlet.2010.09.089
104. S. Li, Y. Li, H. Xiao, X. Li, Q. Wang et al., Oxidation behavior of Si_3N_4 fibers derived from polycarbosilane. Corros. Sci. **136**, 9–17 (2018). https://doi.org/10.1016/j.corsci.2018.02.032
105. F. Li, W. Cui, J. Zhang, S. Du, Z. Chen et al., Synthesis, characterization and growth mechanism of SiC fibers. Mater. Chem. Phys. **291**, 126703 (2022). https://doi.org/10.1016/j.matchemphys.2022.126703
106. Y.K. Chih, J. Hwang, C.S. Kou, C.C. Chuang, J.L. Hu et al., Surface modification of hollow carbon fibres using plasma treatment. Surf. Eng. **27**(8), 623–626 (2011). https://doi.org/10.1179/026708410x12786785573391
107. M. Bonitz, A. Filinov, J.-W. Abraham, K. Balzer, H. Kählert et al., Towards an integrated modeling of the plasma-solid interface. Front. Chem. Sci. Eng. **13**(2), 201–237 (2019). https://doi.org/10.1007/s11705-019-1793-4
108. Z. Yang, X. Huang, J. Li, B. Tang, G. Huang et al., Improved amine functionalization of carbon fiber surfaces by O_2 plasma activation treatment. Compos. Interfaces **30**(12), 1411–1427 (2023). https://doi.org/10.1080/09276440.2023.2223407
109. A. Vesel, M. Mozetic, New developments in surface functionalization of polymers using controlled plasma treatments. J. Phys. D Appl. Phys. **50**(29), 293001 (2017). https://doi.org/10.1088/1361-6463/aa748a
110. L. Xing, L. Liu, Y. Huang, D. Jiang, B. Jiang et al., Enhanced interfacial properties of domestic aramid fiber-12 *via* high energy gamma ray irradiation. Compos. Part B Eng. **69**, 50–57 (2015). https://doi.org/10.1016/j.compositesb.2014.09.027
111. D. Bhattacharyya, V. Baheti, Ozone assisted modification and pulverization of plant fibres. Ind. Crops Prod. **199**, 116711 (2023). https://doi.org/10.1016/j.indcrop.2023.116711
112. H.S. Maqsood, U. Bashir, J. Wiener, M. Puchalski, S. Sztajnowski et al., Ozone treatment of jute fibers. Cellulose **24**(3), 1543–1553 (2017). https://doi.org/10.1007/s10570-016-1164-y
113. Y.V. Tertyshnaya, S.G. Karpova, M.V. Podzorova, Effect of ozone on nonwoven polylactide/natural rubber fibers. Polymers **17**(15), 2102 (2025). https://doi.org/10.3390/polym17152102
114. J. Yu, X. Gao, W. Yang, Z. Zhang, T. Sheng et al., Preparation of nanocarbon-coated glass fibre/phenolic composites for EMI shielding. Bull. Mater. Sci. **45**(3), 116 (2022). https://doi.org/10.1007/s12034-022-02702-8
115. Y. Cheng, K. Wang, Y. Qi, Z. Liu, Chemical vapor deposition method for graphene fiber materials. Acta Phys. Chim. Sin. **38**, 2006046 (2020). https://doi.org/10.3866/pku.whxb202006046
116. X. Luo, S. Wu, Y.-Q. Yang, N. Jin, S. Liu et al., Deposition characteristics of titanium coating deposited on SiC fiber by cold-wall chemical vapor deposition. Mater. Chem. Phys. **184**, 189–196 (2016). https://doi.org/10.1016/j.matchemphys.2016.09.041
117. A. Saffar Shamshirgar, M.F. Álvarez, A. del Campo, J.F. Fernández, R.E. Rojas Hernández et al., Versatile

graphene-alumina nanofibers for microwave absorption and EMI shielding. Carbon **210**, 118057 (2023). https://doi.org/10.1016/j.carbon.2023.118057

118. M. Pitto, H. Fiedler, N.K. Kim, C.J.R. Verbeek, T.D. Allen et al., Carbon fibre surface modification by plasma for enhanced polymeric composite performance: a review. Compos. A Appl. Sci. Manuf. **180**, 108087 (2024). https://doi.org/10.1016/j.compositesa.2024.108087
119. Z. Huang, H. Einaga, Effect of ozone treatment on microwave heating properties of carbon fiber. Catal. Today **458**, 115386 (2025). https://doi.org/10.1016/j.cattod.2025.115386
120. G. Kim, H. Lee, K. Kim, D.U. Kim, Effects of heat treatment atmosphere and temperature on the properties of carbon fibers. Polymers **14**(12), 2412 (2022). https://doi.org/10.3390/polym14122412
121. C. Li, Z. Sun, T. Yang, L. Yu, N. Wei et al., Directly grown vertical graphene carpets as Janus separators toward stabilized Zn metal anodes. Adv. Mater. **32**(33), e2003425 (2020). https://doi.org/10.1002/adma.202003425
122. H.P.L. Gemoets, Y. Su, M. Shang, V. Hessel, R. Luque et al., Liquid phase oxidation chemistry in continuous-flow microreactors. Chem. Soc. Rev. **45**(1), 83–117 (2016). https://doi.org/10.1039/c5cs00447k
123. W.-J. Liu, L. Dang, Z. Xu, H.-Q. Yu, S. Jin et al., Electrochemical oxidation of 5-hydroxymethylfurfural with NiFe layered double hydroxide (LDH) nanosheet catalysts. ACS Catal. **8**(6), 5533–5541 (2018). https://doi.org/10.1021/acscatal.8b01017
124. J. Moosburger-Will, M. Bauer, E. Laukmanis, R. Horny, D. Wetjen et al., Interaction between carbon fibers and polymer sizing: influence of fiber surface chemistry and sizing reactivity. Appl. Surf. Sci. **439**, 305–312 (2018). https://doi.org/10.1016/j.apsusc.2017.12.251
125. Z. Jia, T. Xu, S. Yang, Y. Luo, D. Jia, Interfacial mechanochemical grafting in styrene-butadiene rubber/halloysite nanotubes composites. Polym. Test. **54**, 29–39 (2016). https://doi.org/10.1016/j.polymertesting.2016.06.022
126. P. Purohit, A. Bhatt, R.K. Mittal, M.H. Abdellattif, T.A. Farghaly, Polymer grafting and its chemical reactions. Front. Bioeng. Biotechnol. **10**, 1044927 (2023). https://doi.org/10.3389/fbioe.2022.1044927
127. B. Sudduth, J. Sun, Y. Wang, Chemical grafting of highly dispersed VOx/CeO_2 for increased catalytic activity in methanol oxidative dehydrogenation. Catal. Lett. **152**(10), 2980–2992 (2022). https://doi.org/10.1007/s10562-021-03862-8
128. G. Ni, Y. Yang, K. Chen, C. Liu, S. Wang, Optimization of pore structure and surface chemical properties of activated carbon fiber *via* liquid-phase stabilization for enhanced supercapacitor performance. Diam. Relat. Mater. **149**, 111607 (2024). https://doi.org/10.1016/j.diamond.2024.111607
129. Y. Fu, H. Li, W. Cao, Enhancing the interfacial properties of high-modulus carbon fiber reinforced polymer matrix composites *via* electrochemical surface oxidation and grafting. Compos. Part A Appl. Sci. Manuf. **130**, 105719 (2020). https://doi.org/10.1016/j.compositesa.2019.105719
130. T. Li, Y. Jiang, L. Zeng, H. Zhang, Z. Yuan et al., Surface sizing introducing Fe_3O_4 nanoparticles for magnetic properties strengthening of basalt fibers. Ceram. Int. **51**(2), 2216–2225 (2025). https://doi.org/10.1016/j.ceramint.2024.11.199
131. H. Gupta, P.K. Agnihotri, S. Basu, N. Gupta, Carbon nanotube grafting for better electromagnetic shielding with carbon fiber/epoxy composites. Polym. Compos. **46**(S3), S856–S866 (2025). https://doi.org/10.1002/pc.30003
132. F. Ji, C. Liu, Y. Hu, S. Xu, Y. He et al., Chemically grafting carbon nanotubes onto carbon fibers for enhancing interfacial properties of fiber metal laminate. Materials **13**(17), 3813 (2020). https://doi.org/10.3390/ma13173813
133. H. Lee, M.K. Choi, S.-H. Kang, W. Han, B.-J. Kim et al., Heat-treated Ni-coated fibers for EMI shielding: balancing electrical performance and interfacial integrity. Polymers **17**(12), 1610 (2025). https://doi.org/10.3390/polym17121610
134. X. Li, S. Zhou, Z. Ji, Q. Xu, J. Dong et al., Fabrication of conductive polyimide/metal composite fibers for high temperature EMI shielding. Appl. Surf. Sci. **680**, 161293 (2025). https://doi.org/10.1016/j.apsusc.2024.161293
135. J.-H. Park, C. Cho, K.H. Kim, J.-H. Kang, M.-K. Seo et al., Effect of plating thickness on PA6/nickel-plated carbon fiber composites manufactured using LFT pellets. Polym. Compos. **46**(10), 9576–9585 (2025). https://doi.org/10.1002/pc.29580
136. S. Zhou, J. Dong, X. Li, X. Zhao, Q. Zhang, Continuous surface metallization of polyimide fibers for textile-substrate electromagnetic shielding applications. Adv. Fiber Mater. **5**(6), 1892–1904 (2023). https://doi.org/10.1007/s42765-023-00317-0
137. H. Zhao, L. Hou, Y. Lu, Electromagnetic interference shielding of layered linen fabric/polypyrrole/nickel (LF/PPy/Ni) composites. Mater. Des. **95**, 97–106 (2016). https://doi.org/10.1016/j.matdes.2016.01.088
138. R. Zhang, G. Zhang, S. Zhuang, X. Lu, D. Zhang et al., Flexible Ni-Fe-P/PPy@PI fiber paper-based composites with three-layer structure for 5 G electromagnetic shielding applications. J. Alloys Compd. **897**, 163232 (2022). https://doi.org/10.1016/j.jallcom.2021.163232
139. Y. Duan, X. Fang, Z. Zhang, R. Sun, J. Hong et al., Lightweight, flexible rCEF@PPy/MXene for ultra-efficient EMI shielding felt with Joule heating performance. Mater. Lett. **341**, 134297 (2023). https://doi.org/10.1016/j.matlet.2023.134297
140. D. Zhang, H. Yang, J. Pan, B. Lewis, W. Zhou et al., Multifunctional CNT nanopaper polyurethane nanocomposite fabricated by ultrasonic infiltration and dip soaking processes. Compos. Part B Eng. **182**, 107646 (2020). https://doi.org/10.1016/j.compositesb.2019.107646
141. Y. Shao, L. Zou, Y. Chen, L. Wang, L. Song et al., Core-sheath structured CNT@Ni-CNT fiber-based multifunctional fabric with high-sensitivity, wide-range strain sensing, and enhanced electromagnetic shielding absorption. Chem. Eng. J. **512**, 162358 (2025). https://doi.org/10.1016/j.cej.2025.162358
142. J. Hu, X. Xiong, Y. Chen, H. Long, Design and construction of interface engineering in short carbon fiber composites for

© The authors

excellent mechanical properties and efficient electromagnetic interference shielding. Appl. Surf. Sci. **685**, 162098 (2025). https://doi.org/10.1016/j.apsusc.2024.162098

143. W. Feng, L. Zou, C. Lan, S. E, X. Pu, Core-sheath CNT@MXene fibers toward absorption-dominated electromagnetic interference shielding fabrics. Adv. Fiber Mater. **6**(5), 1657–1668 (2024). https://doi.org/10.1007/s42765-024-00452-2
144. M. Zhou, S. Tan, J. Wang, Y. Wu, L. Liang et al., Three-in-one" multi-scale structural design of carbon fiber-based composites for personal electromagnetic protection and thermal management. Nano-Micro Lett. **15**(1), 176 (2023). https://doi.org/10.1007/s40820-023-01144-z
145. Q. Wang, Y. Wang, C. Sun, Y. Zhang, R. Qu et al., Multifunctional aramid nanofiber/MXene/aramid fiber composite fabric with outstanding EMI shielding performance. Coatings **15**(3), 354 (2025). https://doi.org/10.3390/coatings15030354
146. J. Yu, Z. Cui, J. Lu, J. Zhao, Y. Zhang et al., Integrated hierarchical macrostructures of flexible basalt fiber composites with tunable electromagnetic interference (EMI) shielding and rapid electrothermal response. Compos. Part B Eng. **224**, 109193 (2021). https://doi.org/10.1016/j.compositesb.2021.109193
147. X. Zhang, D. Miao, X. Ning, M. Cai, Y. Tian et al., The stability study of copper sputtered polyester fabrics in synthetic perspiration. Vacuum **164**, 205–211 (2019). https://doi.org/10.1016/j.vacuum.2019.03.023
148. C.L. Xia, H. Ren, S.Q. Shi, H.L. Zhang, J.T. Cheng et al., Natural fiber composites with EMI shielding function fabricated using VARTM and Cu film magnetron sputtering. Appl. Surf. Sci. **362**, 335–340 (2016). https://doi.org/10.1016/j.apsusc.2015.11.202
149. Q. Wang, S. Xiao, S.Q. Shi, S. Xu, L. Cai, Self-bonded natural fiber product with high hydrophobic and EMI shielding performance *via* magnetron sputtering Cu film. Appl. Surf. Sci. **475**, 947–952 (2019). https://doi.org/10.1016/j.apsusc.2019.01.059
150. A. Singh, G. den Van Mooter, Spray drying formulation of amorphous solid dispersions. Adv. Drug Deliv. Rev. **100**, 27–50 (2016). https://doi.org/10.1016/j.addr.2015.12.010
151. S. Huang, M.-L. Vignolles, X.D. Chen, Y. Le Loir, G. Jan et al., Spray drying of probiotics and other food-grade bacteria: a review. Trends Food Sci. Technol. **63**, 1–17 (2017). https://doi.org/10.1016/j.tifs.2017.02.007
152. H. Wang, X. Sun, Y. Wang, K. Li, J. Wang et al., Acid enhanced zipping effect to densify MWCNT packing for multifunctional MWCNT films with ultra-high electrical conductivity. Nat. Commun. **14**(1), 380 (2023). https://doi.org/10.1038/s41467-023-36082-2
153. T. Arunkumar, R. Karthikeyan, R. Ram Subramani, K. Viswanathan, M. Anish, Synthesis and characterisation of multi-walled carbon nanotubes (MWCNTs). Int. J. Ambient Energy **41**(4), 452–456 (2020). https://doi.org/10.1080/01430750.2018.1472657
154. B.-J. Kim, B.K. Deka, I.-J. Bae, D.-H. Choi, D.-I. Son et al., Unidirectional spread-tow carbon fiber/polypropylene composites reinforced with mechanically aligned multi-walled carbon nanotubes and exfoliated graphite nanoplatelets. Polym. Compos. **39**(S2), E1251–E1261 (2018). https://doi.org/10.1002/pc.24835
155. M.-S. Kim, J. Yan, K.-M. Kang, K.-H. Joo, Y.-J. Kang et al., Soundproofing ability and mechanical properties of polypropylene/exfoliated graphite nanoplatelet/carbon nanotube (PP/xGnP/CNT) composite. Int. J. Precis. Eng. Manuf. **14**(6), 1087–1092 (2013). https://doi.org/10.1007/s12541-013-0146-3
156. J.R.N. Gnidakouong, J.-H. Kim, H. Kim, Y.-B. Park, Electromagnetic interference shielding behavior of hybrid carbon nanotube/exfoliated graphite nanoplatelet coated glass fiber composites. Mater. Sci. Eng. B Solid-State Mater. Adv. Technol. **248**, 114403 (2019). https://doi.org/10.1016/j.mseb.2019.114403
157. P. Zhang, I. Wyman, J. Hu, S. Lin, Z. Zhong et al., Silver nanowires: synthesis technologies, growth mechanism and multifunctional applications. Mater. Sci. Eng. B Solid-State Mater. Adv. Technol. **223**, 1–23 (2017). https://doi.org/10.1016/j.mseb.2017.05.002
158. T. Hao, H. Ji, D. Xu, D. Liu, Z. Ren et al., Capillary force-induced graphene spontaneous transfer and encapsulation of silver nanowires for highly-stable transparent electrodes. ACS Appl. Mater. Interfaces **16**(30), 40199–40209 (2024). https://doi.org/10.1021/acsami.4c06315
159. C. Liang, Q. Huo, J. Qi, Y. Zhang, C. Liu et al., Robust solid–solid phase change coating encapsulated glass fiber fabric with electromagnetic interference shielding for thermal management and message encryption. Adv. Funct. Mater. **34**(49), 2409146 (2024). https://doi.org/10.1002/adfm.202409146
160. Y. Yang, W. Chen, Y. Xue, Interfacial bonding within Cu-based composites reinforced with TiC-or Ni-coated carbon fiber. Chin. J. Mater. Res. **35**, 467–473 (2021). https://doi.org/10.11901/1005.3093.2020.357
161. B.-L. Sun, X.-L. Shi, Q. Hu, M. Du, H. Gong et al., Ultra-high-strength textile fiber-supported schiff base copper complexes for photocatalytic degradation of methyl orange. ACS Appl. Polym. Mater. **6**(21), 13077–13088 (2024). https://doi.org/10.1021/acsapm.4c02009
162. Y. Guo, X. Hong, Y. Wang, Q. Li, J. Meng et al., Multi-component hierarchical Cu-doped NiCo-LDH/CuO double arrays for ultralong-life hybrid fiber supercapacitor. Adv. Funct. Mater. **29**(24), 1809004 (2019). https://doi.org/10.1002/adfm.201809004
163. A. Agresti, F. Di Giacomo, S. Pescetelli, A. Di Carlo, Scalable deposition techniques for large-area perovskite photovoltaic technology: a multi-perspective review. Nano Energy **122**, 109317 (2024). https://doi.org/10.1016/j.nanoen.2024.109317
164. J. Feng, Y. Jiao, H. Wang, X. Zhu, Y. Sun et al., High-throughput large-area vacuum deposition for high-performance formamidine-based perovskite solar cells. Energy Environ. Sci. **14**(5), 3035–3043 (2021). https://doi.org/10.1039/d1ee00634g

165. J.H. Koo, J. Kang, S. Lee, J.-K. Song, J. Choi et al., A vacuum-deposited polymer dielectric for wafer-scale stretchable electronics. Nat. Electron. **6**(2), 137–145 (2023). https://doi.org/10.1038/s41928-023-00918-y
166. S. Song, L. Li, D. Ji, J. Zhao, Q. Wu et al., Flexible basalt fiber/aramid nanofiber/carbon nanotube electromagnetic shielding paper with outstanding environmental stability and joule heating performance. ACS Appl. Mater. Interfaces **15**(29), 35495–35506 (2023). https://doi.org/10.1021/acsami.3c06138
167. N. De Greef, L. Zhang, A. Magrez, L. Forró, J.-P. Locquet et al., Direct growth of carbon nanotubes on carbon fibers: effect of the CVD parameters on the degradation of mechanical properties of carbon fibers. Diamond Relat. Mater. **51**, 39–48 (2015). https://doi.org/10.1016/j.diamond.2014.11.002
168. D. Luo, F. Wang, L. Li, Y. Cao, S. Yang et al., Recycling wind turbine blade to fabricate 3D framework for ultra-robust composite with enhanced electromagnetic interference shielding. Compos. Part B Eng. **305**, 112734 (2025). https://doi.org/10.1016/j.compositesb.2025.112734
169. Z. Wang, D. Gong, W. Chen, C. Zhang, A high-sensitivity and fast-recovery strain sensor based on gradient polyurethane and electroless silver-plating on a high aspect ratio glass fibers. Chem. Eng. J. **507**, 160439 (2025). https://doi.org/10.1016/j.cej.2025.160439
170. J. Ruan, Z. Chang, H. Rong, T.S. Alomar, D. Zhu et al., High-conductivity nickel shells encapsulated wood-derived porous carbon for improved electromagnetic interference shielding. Carbon **213**, 118208 (2023). https://doi.org/10.1016/j.carbon.2023.118208
171. L. Xu, R. Si, Q. Ni, J. Chen, J. Zhang et al., Synergistic magnetic/dielectric loss and layered structural design of Ni@carbon fiber/Ag@graphene fiber/polydimethylsiloxane composite for high-absorption EMI shielding. Carbon **225**, 119155 (2024). https://doi.org/10.1016/j.carbon.2024.119155
172. Y. Liu, D. He, O. Dubrunfaut, A. Zhang, L. Pichon et al., *In-situ* growing carbon nanotubes on nickel modified glass fiber reinforced epoxy composites for EMI application. Appl. Compos. Mater. **28**(3), 777–790 (2021). https://doi.org/10.1007/s10443-021-09894-y
173. A. Parkash, A. Kadier, P.-C. Ma, Enhanced EMI shielding performance of glass fiber fabric *via* optimized electroless copper deposition. Mater. Sci. Eng. B **318**, 118333 (2025). https://doi.org/10.1016/j.mseb.2025.118333
174. W. Yang, Y. Fu, A. Xia, K. Zhang, Z. Wu, Microwave absorption property of Ni–Co–Fe–P-coated flake graphite prepared by electroless plating. J. Alloys Compd. **518**, 6–10 (2012). https://doi.org/10.1016/j.jallcom.2011.12.014
175. W. Jang, S. Mallesh, L. Bok, K. Hyeon, Microwave absorption properties of core-shell structured FeCoNi@PMMA filled in composites. Curr. Appl. Phys. **20**(4), 525–530 (2020). https://doi.org/10.1016/j.cap.2020.01.019
176. Q. Wang, Y. Xu, S. Bi, Y. Lu, Enhanced electromagnetic-interference shielding effectiveness and mechanical strength of Co-Ni coated aramid-carbon blended fabric. Chin. J. Aeronaut. **34**(10), 103–114 (2021). https://doi.org/10.1016/j.cja.2021.03.011
177. Y. Wang, J. Wang, Z. Liu, S. Zheng, W. Lu et al., Nanocone-shaped Ni-electroplated carbon fiber composite films for electromagnetic shielding applications. J. Mater. Res. Technol. **27**, 4625–4632 (2023). https://doi.org/10.1016/j.jmrt.2023.10.216
178. A. Bhattacharya, A. De, Conducting composites of polypyrrole and polyaniline a review. Prog. Solid State Chem. **24**(3), 141–181 (1996). https://doi.org/10.1016/0079-6786(96)00002-7
179. M. Beygisangchin, S. Abdul Rashid, S. Shafie, A.R. Sadrolhosseini, H.N. Lim, Preparations, properties, and applications of polyaniline and polyaniline thin films-a review. Polymers **13**(12), 2003 (2021). https://doi.org/10.3390/polym13122003
180. Q. Meng, K. Cai, Y. Chen, L. Chen, Research progress on conducting polymer based supercapacitor electrode materials. Nano Energy **36**, 268–285 (2017). https://doi.org/10.1016/j.nanoen.2017.04.040
181. Y. Wu, Z. Wang, X. Liu, X. Shen, Q. Zheng et al., Ultralight graphene foam/conductive polymer composites for exceptional electromagnetic interference shielding. ACS Appl. Mater. Interfaces **9**(10), 9059–9069 (2017). https://doi.org/10.1021/acsami.7b01017
182. X. He, C. Cui, Y. Chen, L. Zhang, X. Sheng et al., MXene and polymer collision: sparking the future of high-performance multifunctional coatings. Adv. Funct. Mater. **34**(51), 2409675 (2024). https://doi.org/10.1002/adfm.202409675
183. J. Luo, Y. Xue, C. Yang, Y. Liu, L. Zhang et al., Core-shell BN/SCF architecture with phonon-electronic dual conduction pathways for synergistic enhancement of thermal conductivity, EMI shielding and mechanical properties in CF/EP composites. Compos. Part B Eng. **305**, 112747 (2025). https://doi.org/10.1016/j.compositesb.2025.112747
184. M. Ma, Z. Liao, X. Su, Q. Zheng, Y. Liu et al., Magnetic CoNi alloy particles embedded N-doped carbon fibers with polypyrrole for excellent electromagnetic wave absorption. J. Colloid Interface Sci. **608**(Pt 3), 2203–2212 (2022). https://doi.org/10.1016/j.jcis.2021.10.006
185. Y. Gou, H. Wen, W. Zhang, A promising CF@PANI multifunctional absorbents: preparation and microwave absorption performance investigation. Mater. Res. Bull. **192**, 113610 (2025). https://doi.org/10.1016/j.materresbull.2025.113610
186. C. Chang, X. Yue, B. Hao, D. Xing, P.-C. Ma, Direct growth of carbon nanotubes on basalt fiber for the application of electromagnetic interference shielding. Carbon **167**, 31–39 (2020). https://doi.org/10.1016/j.carbon.2020.05.074
187. Q. Men, S. Wang, Z. Yan, B. Zhao, L. Guan et al., Iron-encapsulated CNTs on carbon fiber with high-performance EMI shielding and electrocatalytic activity. Adv. Compos. Hybrid Mater. **5**(3), 2429–2439 (2022). https://doi.org/10.1007/s42114-022-00457-8
188. N. Yamamoto, R. de Guzman Villoria, B.L. Wardle, Electrical and thermal property enhancement of fiber-reinforced polymer laminate composites through controlled implementation of multi-walled carbon nanotubes. Compos. Sci. Technol.

© The authors

72(16), 2009–2015 (2012). https://doi.org/10.1016/j.compscitech.2012.09.006

189. W. Li, F. Liang, X. Sun, K. Zheng, R. Liu et al., Graphene-skinned alumina fiber fabricated through metalloid-catalytic graphene CVD growth on nonmetallic substrate and its mass production. Nat. Commun. **15**(1), 6825 (2024). https://doi.org/10.1038/s41467-024-51118-x
190. F. Liang, W. Li, K. Zheng, K. Huang, S. Cheng et al., Graphene-skinned alumina fiber fabric for diverse electrothermal and electromagnetic compatibility and its mass production. Adv. Mater. **37**(28), 2501226 (2025). https://doi.org/10.1002/adma.202501226
191. X. Gao, Q. Zhou, J. Wang, L. Xu, W. Zeng, Performance of intrinsic and modified graphene for the adsorption of H_2S and CH_4: a DFT study. Nanomaterials **10**(2), 299 (2020). https://doi.org/10.3390/nano10020299
192. K. Pirabul, Q. Zhao, Z.-Z. Pan, H. Liu, M. Itoh et al., Silicon radical-induced CH_4 dissociation for uniform graphene coating on silica surface. Small **20**(16), e2306325 (2024). https://doi.org/10.1002/smll.202306325
193. K. Zheng, C. Yu, W. Li, F. liang, L. Liu et al., Rapid preparation of graphene-skinned alumina fiber fabric and its electromagnetic interference shielding application. Nano Res. **18**(5), 94907330 (2025). https://doi.org/10.26599/nr.2025.94907330
194. G. Zhang, J. Yu, C. Su, C. Di, S. Ci et al., The effect of annealing on the properties of copper-coated carbon fiber. Surf. Interface. **37**, 102630 (2023). https://doi.org/10.1016/j.surfin.2023.102630
195. Z. Wang, G. Cai, Y. Xia, P. Li, S. Shi et al., Highly conductive graphene fiber textile for electromagnetic interference shielding. Carbon **222**, 118996 (2024). https://doi.org/10.1016/j.carbon.2024.118996
196. X. Gao, X. Wang, J. Cai, Y. Zhang, J. Zhang et al., CNT cluster arrays grown on carbon fiber for excellent green EMI shielding and microwave absorbing. Carbon **211**, 118083 (2023). https://doi.org/10.1016/j.carbon.2023.118083
197. B. Wu, G. Qian, Y. Yan, M.M. Alam, R. Xia et al., Design of interconnected carbon fiber thermal management composites with effective EMI shielding activity. ACS Appl. Mater. Interfaces **14**(43), 49082–49093 (2022). https://doi.org/10.1021/acsami.2c13433
198. Y. Xing, Y. Wan, Z. Wu, J. Wang, S. Jiao et al., Multilayer ultrathin MXene@AgNW@MoS_2 composite film for high-efficiency electromagnetic shielding. ACS Appl. Mater. Interfaces **15**(4), 5787–5797 (2023). https://doi.org/10.1021/acsami.2c18759
199. L. Li, Q. Cheng, MXene based nanocomposite films. Exploration **2**(4), 20220049 (2022). https://doi.org/10.1002/exp.20220049
200. Y.-J. Choi, S.C. Gong, D.C. Johnson, S. Golledge, G.Y. Yeom et al., Characteristics of the electromagnetic interference shielding effectiveness of Al-doped ZnO thin films deposited by atomic layer deposition. Appl. Surf. Sci. **269**, 92–97 (2013). https://doi.org/10.1016/j.apsusc.2012.09.159
201. X. Wan, Y. Zhao, Z. Li, L. Li, Emerging polymeric electrospun fibers: from structural diversity to application in flexible bioelectronics and tissue engineering. Exploration **2**(1), 20210029 (2022). https://doi.org/10.1002/EXP.20210029
202. A. He, Y. Luo, M. Wang, Y. Zhang, Z. Huang et al., Pearl-inspired colored carbon fibers with electromagnetic interference and optical camouflage properties. Energy Environ. Mater. **8**(2), e12840 (2025). https://doi.org/10.1002/eem2.12840
203. P.G. Gordon, G. Bačić, G.P. Lopinski, S.T. Barry, Work function of doped zinc oxide films deposited by ALD. J. Mater. Res. **35**(7), 756–761 (2020). https://doi.org/10.1557/jmr.2019.334
204. G. Lin, T. Zhou, Z. Zhou, W. Sun, Laser induced graphene for EMI shielding and ballistic impact damage detection in basalt fiber reinforced composites. Compos. Sci. Technol. **242**, 110182 (2023). https://doi.org/10.1016/j.compscitech.2023.110182
205. X. Tang, X. Yan, Dip-coating for fibrous materials: mechanism, methods and applications. J. Sol-Gel Sci. Technol. **81**(2), 378–404 (2017). https://doi.org/10.1007/s10971-016-4197-7
206. J. Wu, X. Zhao, C. Tang, J. Lei, L. Li, One-step dipping method to prepare inorganic-organic composite superhydrophobic coating for durable protection of magnesium alloys. J. Taiwan Inst. Chem. Eng. **135**, 104364 (2022). https://doi.org/10.1016/j.jtice.2022.104364
207. S.J. Pothupitiya Gamage, K. Yang, R. Braveenth, K. Raagulan, H.S. Kim et al., MWCNT coated free-standing carbon fiber fabric for enhanced performance in EMI shielding with a higher absolute EMI SE. Materials **10**(12), 1350 (2017). https://doi.org/10.3390/ma10121350
208. X. Mei, L. Lu, Y. Xie, Y.-X. Yu, Y. Tang et al., Preparation of flexible carbon fiber fabrics with adjustable surface wettability for high-efficiency electromagnetic interference shielding. ACS Appl. Mater. Interfaces **12**(43), 49030–49041 (2020). https://doi.org/10.1021/acsami.0c08868
209. Y. Zhang, G. Shen, S.S. Lam, S. Ansar, S.-C. Jung et al., A waste textiles-based multilayer composite fabric with superior electromagnetic shielding, infrared stealth and flame retardance for military applications. Chem. Eng. J. **471**, 144679 (2023). https://doi.org/10.1016/j.cej.2023.144679
210. M. Qi, G. Xiao, S. Chen, X. Wang, A. Duan et al., Modification of a chromogenic inorganic basalt fabric *via* a functionalized anthraquinone polyurethane mixed coating: exceptional wear resistance and EMI shielding. ACS Appl. Polym. Mater. **7**(19), 13415–13427 (2025). https://doi.org/10.1021/acsapm.5c03050
211. G. Yu, G. Shao, Z. Xu, Y. Chen, X. Huang, Hierarchical interface-engineered magnetic graphene-sicn aerogels *via* stepwise confinement strategy for low-frequency and broadband microwave absorption. J. Adv. Ceram. (2025). https://doi.org/10.26599/jac.2025.9221187
212. G. Yu, G. Shao, R. Xu, Y. Chen, X. Zhu et al., Metal-organic framework-manipulated dielectric genes inside silicon carbonitride toward tunable electromagnetic wave absorption.

Small **19**(46), e2304694 (2023). https://doi.org/10.1002/smll.202304694

213. G. Yu, G. Shao, Y. Chen, Z. Xu, B. Quan et al., Intelligent hygroscopic aerogels: moisture-activated dual-mode switchable electromagnetic response. Adv. Funct. Mater. **35**(42), 2506857 (2025). https://doi.org/10.1002/adfm.202506857
214. X. Huang, G. Yu, B. Quan, J. Xu, G. Sun et al., Harnessing pseudo-jahn-teller disordering of monoclinic birnessite for excited interfacial polarization and local magnetic domains. Small Methods **7**(9), e2300045 (2023). https://doi.org/10.1002/smtd.202300045
215. X. Huang, J. Wei, Y. Zhang, B. Qian, Q. Jia et al., Ultralight magnetic and dielectric aerogels achieved by metal-organic framework initiated gelation of graphene oxide for enhanced microwave absorption. Nano-Micro Lett. **14**(1), 107 (2022). https://doi.org/10.1007/s40820-022-00851-3
216. J. Liang, S. Zhu, D. Chen, Y. Li, D. Zhou et al., Dual built-in electric field engineering in heterostructure nickel-cobalt bimetallic composites for boosted electromagnetic energy dissipation. Adv. Powder Mater. **4**(6), 100344 (2025). https://doi.org/10.1016/j.apmate.2025.100344
217. X. Huang, J. Guan, Y. Feng, Q. Zhang, B. Quan et al., Mn and O defect modulation in birnessite creates multiplicate polyhedra to improve dielectric and magnetic losses. Cell Rep. Phys. Sci. **6**(1), 102350 (2025). https://doi.org/10.1016/j.xcrp.2024.102350
218. Z. Liu, J. Liu, H. bian, X. Zhou, H. Liang et al., Lattice expansion/contraction triggered by etching-assisted strain engineering of cobalt sulfide heterostructures to boost electromagnetic wave absorption. Adv. Powder Mater. **5**(2), 100367 (2026). https://doi.org/10.1016/j.apmate.2025.100367
219. Y. Wan, J. Xiao, C. Li, G. Xiong, R. Guo et al., Microwave absorption properties of FeCo-coated carbon fibers with varying morphologies. J. Magn. Magn. Mater. **399**, 252–259 (2016). https://doi.org/10.1016/j.jmmm.2015.10.006
220. S. Liu, J. Wang, B. Zhang, X. Su, X. Chen et al., Transformation of traditional carbon fibers from microwaves reflection to efficient absorption via carbon fiber microstructure modulation. Carbon **219**, 118802 (2024). https://doi.org/10.1016/j.carbon.2024.118802

Publisher's Note Springer Nature remains neutral with regard to jurisdictional claims in published maps and institutional affiliations.